GEORGIA DOT RESEARCH PROJECT 17-32

Final Report

VALIDATING CHANGE OF SIGN AND PAVEMENT CONDITIONS AND EVALUATING SIGN RETROREFLECTIVITY CONDITION ASSESSMENT ON GEORGIA'S INTERSTATE HIGHWAYS USING 3D SENSING TECHNOLOGY

GDOT
Georgia Department of Transportation

Office of Performance-based Management and Research
600 West Peachtree St. NW | Atlanta, GA 30308

1.Report No.: FHWA-GA-20-1732	2. Government Accession No.: N/A	3. Recipient's Catalog No.: N/A
4. Title and Subtitle: Validating Change of Sign and Pavement Conditions and Evaluating Sign Retroreflectivity Condition Assessment on Georgia's Interstate Highways Using 3D Sensing Technology		5. Report Date: November 2019
		6. Performing Organization Code: N/A
7. Author(s): Yichang (James) Tsai, Ph.D.; Zhaohua Wang, Ph.D.		8. Performing Organ. Report No.: 17-32
9. Performing Organization Name and Address: Georgia Institute of Technology 790 Atlantic Drive Atlanta, GA 30332-0355		10. Work Unit No.:
		11. Contract or Grant No.: PI# A180701
12. Sponsoring Agency Name and Address: Georgia Department of Transportation Office of Performance-based Management and Research 600 West Peachtree St. NW Atlanta, GA, 30308		13. Type of Report and Period Covered: Final; December 2017 – November 2019
		14. Sponsoring Agency Code:
15. Supplementary Notes:		

16. Abstract:

Traffic signs are important for roadway safety and provide critical guidance to road users with traffic regulations, road hazard warnings, destination information, and other geographic information. Pavement surface distress data is critical for monitoring the statewide pavement conditions, identifying maintenance activities, and optimally allocating pavement funds. In 2015, the Georgia Department of Transportation (GDOT) implemented a comprehensive sign inventory and asphalt pavement condition assessment on Georgia's interstate highways through a research project (RP 15-11). To track the existence and condition change of signs, a new procedure was developed by utilizing the existing sign inventory and condition data. Meanwhile, a sign retro-reflectivity condition assessment method using mobile LiDAR was explored, and a case study was developed to demonstrate the use of the proposed method. The asphalt pavement condition of interstate highways was updated using newly collected 3D pavement laser data. In addition, the condition data of jointed plain concrete pavement (JPCP) and international roughness index (IRI) on interstate highways were collected for this project using the 3D pavement laser data.

17. Key Words: Interstate; Sign Inventory; PACES; Image; Mobile LiDAR; 3D Laser		18. Distribution Statement: No Restriction	
19. Security Classification (of this report): Unclassified	20. Security classification (of this page): Unclassified	21. Number of Pages: 141	22. Price: Free

Contract Research

GDOT Research Project No. 17-32
Final Report

VALIDATING CHANGE OF SIGN AND PAVEMENT CONDITIONS AND EVALUATING SIGN RETROREFLECTIVITY CONDITION ASSESSMENT ON GEORGIA'S INTERSTATE HIGHWAYS USING 3D SENSING TECHNOLOGY

By

Yichang (James) Tsai, Ph.D., P.E.

Zhaohua Wang, Ph.D., P.E.

Georgia Institute of Technology

Contract with

Georgia Department of Transportation

In cooperation with

U.S. Department of Transportation

Federal Highway Administration

November 2019

TABLE OF CONTENTS

LIST OF TABLES

LIST OF FIGURES

ACKNOWLEDGEMENTS

EXECUTIVE SUMMARY

Traffic signs are important for roadway safety and provide critical guidance to road users with traffic regulation, road hazard warnings, destination information, and other geographic information. To better manage and maintain all traffic signs, each state department of transportation (DOT) must perform a comprehensive inventory, track the change of sign conditions, and assess sign retroreflectivity conditions. The Georgia Department of Transportation (GDOT) has implemented a comprehensive sign inventory on Georgia's interstate highways in 2016 through a research project (RP 15-11) performed by the Georgia Institute of Technology (Georgia Tech). Mobile light detection and ranging (LiDAR) and video log images were employed for sign data collection, along with a semi-automatic sign inventory procedure. Pavement surface distress data is critical for monitoring the statewide pavement conditions, identifying maintenance activities, and optimally allocating pavement funds. To validate the use of 3D pavement laser data for pavement distress data collection, the Office of Maintenance (OM) has worked with Georgia Tech to conduct a comprehensive Pavement Condition Evaluation System (PACES) data collection on interstate highways through the above research project.

To track the existence and condition change of signs on interstate highways, this project conducted a sign and pavement condition data inventory again. To utilize the previous sign inventory data, a new procedure was developed, which is much faster than the original process. Sign retroreflectivity conditions are critical for nighttime driving safety.

In GDOT's current practice, nighttime visual inspection is applied to assess sign retroreflectivity conditions; which is subjective, inaccurate, and time- consuming. This project explored a sign retro-reflectivity condition assessment method using mobile LiDAR and validated the proposed method by using a case study.

To track the changes in pavement surface distresses, the asphalt pavement condition evaluation on the interstate highway was conducted again. Other than the PACES data, data on the conditions of jointed plain concrete pavements (JPCP) on interstate highways and the international roughness index (IRI) were also collected in this project using 3D laser data.

The following observations summarize the major findings.

Sign inventory and condition assessment:

- 21,427 traffic signs were inventoried in 2018 along all the interstate highways using a procedure that makes use of previously collected data (2015 sign inventory). The guide signs make up 65% (13,969 signs) of the total sign population on the interstate. The rest of the population consists of 4,465 regulatory signs, 2,717 warning signs, and 276 other signs (temporary signs and signs with no identifiable MUTCD codes).
- There are 1,256 signs (6% of the overall traffic sign population) in poor conditions (such as surface failure, post failure, obstructed by vegetation, and dirty) that require maintenance actions. Surface failure of the signs make up the largest number of signs in poor condition in 2018; this is followed by signs that are dirty. The next two cases are signs that are obstructed, and signs whose posts failed. Further studies are needed

to determine the number of poor condition signs in 2015 that were not repaired until 2018 and to determine the number of additional signs that dropped into poor condition

- There are 4,135 overhead signs (19% of the overall traffic sign population). They have a high potential risk of failure and require frequent monitoring and condition assessment.

- There is an increase of 1.87% in the number of signs in the 2018 Sign Inventory compared to the 2015 Sign Inventory. The largest increase in a number of signs falls under regulatory signs (4%, 188 signs). One of the noted reasons for change in this category comes from the "Prohibited. Holding Mobile Devices While Driving" signs. These signs were installed after 2015 when the state of Georgia passed the Hands-Free Georgia Law (HB673).

<u>Sign retro-reflectivity condition assessment:</u>

- A new method was developed to assess the sign retro-reflectivity condition category (good, poor, and uncertain) using the sign's point cloud data collected by the mobile LIDAR technology. The two main steps involved in this method are 1) computing the retro intensity statistics (such as median and 25th percentile) for the sign point cloud data, and 2) classifying the sign retro-reflectivity condition category (good, poor, uncertain) based on the proposed minimum retro-intensity (MR) criteria.

- The proposed method was validated using the nighttime visual inspection using signs collected from GDOT. The assessment was performed by a GDOT inspector who

classified the signs as "acceptable" or "unacceptable" based on the retro-reflectivity. All the signs that were failed by nighttime visual assessment method were correctly classified as "poor" by the proposed method; among the signs that passed, three signs were categorized as "uncertain" due to localized defects on the sign, such as dirt, cracking, or graffiti.

- A case study was performed on I-285 to assess the feasibility of the proposed method by collecting LIDAR data on selected interstate traffic signs. Among 338 selected signs, 67% of the signs were classified in a good retro-reflectivity condition, and 33 percent of the signs were classified in a "poor" or "uncertain" retro-reflectivity condition.

- A study was conducted to assess the retro-reflectivity deterioration behavior of a few selected signs using the retro-intensity data collected on them over the past 4 years. Promising trends for retro-intensity behavior change can be observed on a these signs. However, due to the unpredictable factors of dirt accumulation, rains, and cleaning of signs by the maintenance crews, the deterioration trends may not be consistent for all the signs in the field. Therefore, it is recommended that the retro-intensity deterioration analysis be performed under controlled conditions (clean the signs before retro-intensity measurement) to yield more consistent results.

Asphalt Pavement Condition Assessment:

- The COPACES ratings were computed for 1,289 miles of asphalt pavement by using the streamlined method for asphalt pavement condition evaluation.

- Overall, the pavement condition on interstate highways in Georgia is relatively acceptable, except for a few sections. The project ratings range from a low of 60 to a high of 99, with an average rating of 82 for all projects. There are 16 projects with a rating of 70 or below.

- The overall deduct value related to load cracking and block cracking are relatively low, most of them being below 6 points, indicating that a low extent and low severity level is mostly identified along the surveyed pavements. Similarly, the rutting deduct values were mostly below 5 points, indicating average rutting of below ¼ inches. However, raveling is the major contributor to the project rating reduction with around 75% of the projects having a raveling deduct value of 10% or above, which indicated more than 36% extent of Severity Level 1, or more than 15% at Severity Level 2.

PCC (JPCP) Pavement Condition Assessment:

- The JPCP ratings (JPCPACES) were computed for a total of 988 survey segments, and each segment represented 1 mile. The overall JPCP condition on Georgia's interstate highway is relatively acceptable with an average rating of 83.7 for all segments. There are 178 segments with a rating below 70 that potentially need maintenance or replacement. The poor performance JPCP pavements are located on I-75 north of Atlanta, I-20 west of Atlanta, I-20 east of Atlanta from MP130-MP150, I-16 near Macon, and I-16 from MP 80-MP 90.

- The deduct value for the faulting index is highly correlated to the deduct value for the IRI, which indicates the faulting index highly impacts the roadway's ride quality.

Moreover, it is found that the high deduct value for longitudinal cracks was mostly concentrated on I-20 west of Atlanta. The high deduct value for shattered slabs was evenly distributed in all the segments with low JPCPACES ratings.

Smoothness Evaluation:

- The validation of the method for IRI measurement was conducted by comparison of IRI values obtained using the Georgia Tech Sensing Van (GTSV) and a GDOT Profiler on two GDOT test sections. First, the repeatability test by the GTSV resulted in a high correlation between any two runs, with an average correlation of 0.7912 for the left wheel path and 0.7876 for the right wheel path. Second, the difference of the average IRI collected by the GTSV and the GDOT Profiler is -0.58 in/mi for the left wheel path and 2.57 in/mi for the right wheel path, which shows high accuracy of IRI measurement using the GTSV.

- The GTSV data from 2017 and 2018 were compared with the data collected by Pathway on I-85 northbound (MP 34-57). The average standard deviation between the IRI values estimated for each mile was 4.65 in/mi, with the highest standard deviation occurring at MP 41-42 of 9.51 in/mi.

- The HRI was processed for all the interstate routes collected by the GTSV, including both asphalt and concrete pavements. Seventy-eight percent of the interstate fell into the "Very Good" and "Good" categories according to the FHWA definition with an HRI value of less than 76 in/mile, with few exceptions of higher HRI, mainly on I-16.

The following are implementation recommendations.

Sign Inventory and Condition Assessment

1) GDOT can take proactive action using the research outcomes from this project to locate and perform timely maintenance for the signs in poor condition in each district. Based on the sign inventory outcomes, along with conditions, it is recommended that GDOT districts use the research outcomes (different categories of poor sign conditions and their locations) to actively perform maintenance and replacement to ensure roadway safety. If the districts are limited by resources for maintenance, it is recommended they perform the maintenance and replacement on the regulatory signs first.

2) GDOT can also use the collected interstate highway sign inventory from this research project to assist the GDOT Office of Transportation Data (OTD) in performing QA/QC on the current statewide sign inventory effort.

3) From the results of I-285 case study on selected signs, we can clearly see that GDOT can potentially reduce sign retro-reflectivity condition assessment effort by approximately 60% on I-285 by screening out the "good" retro-reflectivity signs. GDOT inspectors may only need to assess the remaining 40% of signs in the "poor" and "uncertain" categories to determine if they require replacement or cleaning. To validate the accuracy of the results, it is recommended that GDOT verify the research outcomes from the I-285 case study by assessing the selected signs in the field with its inspectors and perform cleaning or replacement actions on the signs that were identified as "poor" or "uncertain."

4) It is further recommended that GDOT implement the sign retro-reflectivity condition assessment as proposed in this research project at the network-level using the safe, cost-effective mobile-LiDAR data collected at highway speed after the field validation.

Pavement Condition Assessment

1) Knowing that GDOT has a new production operation with an outsourced, automated collection method using 3D sensing technology, it is recommended that a quality assurance procedure be developed to ensure the data quality needed to support the MR&R decision-making. Validating the accuracy and reliability of the GTSV in pavement condition evaluation shows a great potential for use by GDOT as a rigorous method to evaluate the data quality provided by the vendors as part of the data quality management plan.

2) It is recommended that the high granularity of 3D pavement surface data be leveraged not only for evaluating the network condition, but also for maintenance and rehabilitation decisions at the project level. For example, 100-ft aggregated pavement distresses can be obtained and used for determining coring locations required by the Office of Materials and Testing for pavement design evaluation. Moreover, this data can also be used to define optimal termini for localized maintenance applications, such as deep patching of asphalt pavements, or be used to estimate the quantity of broken slab replacements for JPCP needed.

3) Because of having accurate pavement condition data, it is recommended this 3D and pavement distress data be used to better study pavement deterioration behavior and develop a reliable pavement performance forecasting model. For example, a raveling deterioration and forecasting study can be developed to improve GDOT's predictive and preventive maintenance, such as fog seal, micro-milling, and thin overlay optimal timing. Similarly, the slab-level pavement distresses of JPCP can be used to study the change of slab conditions and develop accurate forecasting models to support MR&R decisions, including broken slab replacement.

4) After validating the IRI accuracy collected by the GTSV, it is recommended that GDOT use 3D pavement data, already collected for measurement of cracking, rutting, etc. to compute IRI to reduce the additional effort and cost required to compute IRI data using the laser profilers.

CHAPTER 1.   INTRODUCTION

RESEARCH BACKGROUND AND RESEARCH NEED

Traffic signs are important for roadway safety and provide critical guidance to road users with traffic regulation, road hazard warnings, destination information, and other geographic information. To better manage and maintain all traffic signs, each state department of transportation (DOT) must perform a comprehensive inventory, track the change of sign conditions, and assess sign retroreflectivity conditions. With enough sign condition data over time, a data-driven deterioration model can then be developed, which will help a state DOT allocate its budget for sign maintenance and replacement in a more cost-effective way.   The Georgia DOT (GDOT) implemented a comprehensive sign inventory on Georgia's interstate highways in 2016 through a research project (RP 15-11) performed by the Georgia Institute of Technology (Georgia Tech) (Tsai et al., 2017). Mobile light detection and ranging (LiDAR) and video log images were employed for sign data collection and used along with a semi-automatic sign inventory procedure. There are total 22,344 traffic signs that were inventoried. Among all the signs, 4% of the signs (i.e., 897 signs) were in poor conditions (surface failure, dirty, failed post, or obstructed) to different extents. Using mobile LiDAR and videolog images for sign inventory has proved to be a safer, faster, and more cost-effective approach than the manual, visual inspection method, especially on high-traffic-volume interstate highways.

Pavement surface distress data is critical for monitoring the statewide pavement conditions, identifying maintenance activities, and optimally allocating pavement funds.

To validate the use of 3D laser data for pavement distress data collection, the Office of Maintenance (OM) has worked with Georgia Tech to conduct a comprehensive Pavement Condition Evaluation System (PACES) data collection on interstate highways. The County Pavement Condition System (COPACES) ratings and distresses were collected on 1,513 interstate highway pavement segments. In addition, other than the representative pavement cracking data (in a 100-ft sample section), the full-coverage of distress data was acquired using the automatic distress data collection method and 3D laser technology. The new pavement condition data is an excellent supplement to GDOT's current COPACES survey, which is conducted by using a manual, visual inspection method. For safety concerns, it is difficult, sometimes infeasible, to conduct a manual COPACES survey on a high-traffic-volume interstate highway. Therefore, the automatic pavement distress data collection using 3D laser technology is used because it has proved to be a safer, more accurate, and more cost-effective method than the commonly used manual method, especially on interstate highways that have high volumes of traffic.

To track the existence and condition change of signs and pavement surface distresses on interstate highways, there is a need to conduct sign and pavement condition data inventory again. In the meantime, unlike a new inventory process, the second round of data collection should be faster and more accurate because the sign inventory has been previously done. In the second round, the previous sign inventory data can be utilized to speed up the data collection in the second round and to control the second-round data quality. Other than the PACES data, the conditions of jointed plain concrete pavement (JPCP) on interstate highways and the international roughness index (IRI) will also be

collected in this project using 3D laser data. Based on the discussion with OM and the Office of Research (OR), all interstate highways in Georgia are selected, again, for this case study.

Sign retroreflectivity conditions are critical for nighttime driving safety. In GDOT's current practice, nighttime visual inspection is applied to assess sign retroreflectivity conditions, but the process is subjective, inaccurate, and time consuming. Through the national demonstration project, RP 12-10, entitled "A Remote Sensing and GIS-enabled Asset Management System (RS-GAMS)" that was sponsored by the USDOT and GDOT, the Georgia Tech research team proposed a systematic approach to assess sign retroreflectivity conditions using mobile LiDAR. Compared to the nighttime visual inspection method, the proposed method is more objective, more accurate, and faster. Based on the discussion with OM and OR, the mobile-LiDAR-based sign retroreflectivity condition assessment will be tested in this research project. Though exact reflectivity value is difficult to be acquired from LiDAR retro-intensity data, the proposed approach is capable of categorizing signs as "good," "poor," or "uncertain." The category of "uncertain" means a sign's retroreflectivity condition is marginal and needs an engineer's validation.

RESEARCH OBJECTIVES

The objective of this research project is to conduct the following sign inventory and pavement condition assessment on Georgia's interstate highways: 1) to validate the change of sign inventory, 2) to evaluate sign retroreflectivity conditions using mobile LiDAR, 3) to assess asphalt pavement conditions, 4) to assess JPCP conditions, and 5) to

evaluate pavement smoothness. A new automatic data collection procedure will be

validated using previously collected sign data, including their conditions. It is hoped that

the new method will enhance the sign data collection efficiency and accuracy. In

addition, the proposed sign retroreflectivity condition assessment method using mobile

LiDAR will be validated. The sign inventory includes sign locations, sign types, the

Manual on Uniform Traffic Control Devices (MUTCD) codes, and sign conditions based

on the GDOT Foreman's Manual. A sign's retroreflectivity condition will be categorized

as "pass," "fail," or "uncertain." COPACES data includes 10 types of pavement

distresses that are defined in the PACES manual. In addition, JPCP condition and

pavement IRI data will also be collected in this project.

REPORT ORGANIZATION

This report is organized as follows. CHAPTER 1 presents the background and objective

of the study. CHAPTER 2 overviews the sensing data collection conducted in this study

on the interstate highway system in Georgia. 0 presents a procedure to create an updated

sign inventory using previous sign inventory data. 0 presents a sign retro-reflectivity

condition assessment method using LiDAR technology. CHAPTER 5 presents the results

for asphalt pavement condition assessment. 0 presents the results for JPCP condition

assessment. CHAPTER 7 presents the results for IRI evaluation.   CHAPTER 8

summarizes the findings and discusses the recommendations for implementation.

CHAPTER 2.   OVERVIEW OF THE SENSING DATA COLLECTION

The Georgia Tech Sensing Vehicle (GTSV) was employed in the research project to collect the field roadway videolog images and 3D pavement data. In the final report of a previous research project (RP 15-11), the sensing system was introduced. However, to make this final report a self-contained one, this chapter reiterates the employed sensing system.

GEORGIA TECH SENSING VEHICLE (GTSV)

The GTSV, originally integrated into the national demonstration project performed by the Georgia Tech research team, is introduced in the data collection in this study. Two major subsystems were integrated into the GTSV, including the mobile imaging sub-system for traffic sign inventory and the 3D line laser sub-system for the pavement condition data collection.

The mobile imaging sub-system used in this project consists of three primary components: the LiDAR sensor, the precise positioning system, and the camera system. The LiDAR sensor is used to acquire the point cloud of the target, e.g. a traffic sign. Each point includes the accurate distance from the sensor to the target, the relative angle of the laser beam with respect to the LiDAR sensor, and the corresponding reflectance intensity. The precise positioning system is used to acquire accurate global positioning system (GPS) coordinates and poses for the LiDAR sensor. Thus, the GPS coordinates of each point from the LiDAR sensor can be derived. The positioning system is composed of a

GPS, an inertial measurement unit (IMU), and a distance measurement instrument (DMI) to acquire the precise GPS coordinates. The camera system is synchronized with the LiDAR sensor to provide corresponding color images. **Figure 2-1** illustrates the mobile imaging sub-system on the GTSV.

Figure 2-1. Photo. Mobile imaging sub-system on GTSV.

The current LiDAR sensor can produce 10,000 laser points per second. As the vehicle moves in the longitudinal direction, the scanning line of the LiDAR system is aligned perpendicularly to the ground. The scanning range is ±40° to the horizontal direction, which produces an 80° fan covering the roadside. For example, if a standard 48 in. × 60 in. speed limit sign is mounted on the roadside with a lateral offset of 12 ft. to the edge of the road, the current configuration will be able to acquire a point cloud containing approximately 12×8 points at 60 mph (100 km/h). Based on the previous study, the frequency of the LiDAR system is configured at 100 Hz and 100 points within each scan, while the LiDAR heading angle is configured at 20°. Such a configuration was carefully recommended in the previous study for better acquiring the traffic sign data (Ai & Tsai, 2015). The three video cameras (i.e., front right, front center, and front left camera) are synchronized and calibrated with the LiDAR sensor so that the corresponding 2-D images

can be integrated with the 3D LiDAR point cloud in the same location-referencing

coordinates. The data collection interval of 5 meters is used for collecting the video log

images; this was recommended in the previous study for optimizing the data storage with

sufficient overlap in the video log image sequence (Ai & Tsai, 2015). **Figure 2-2** shows

an illustration of the collected sensing data using the mobile imaging sub-system.
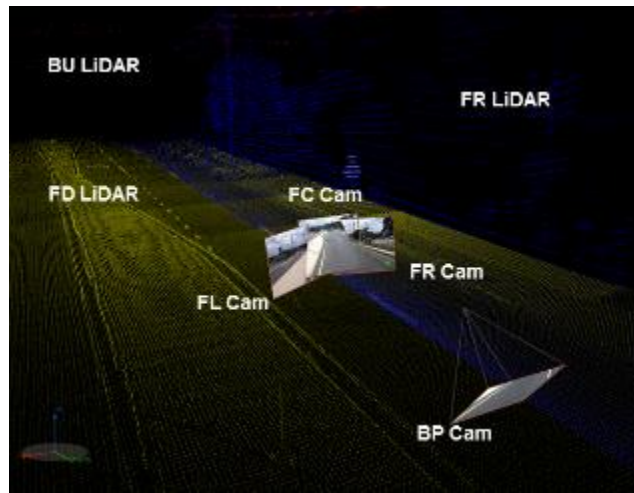
Figure 2-2. Photo. Illustration of the collected sensing data using the mobile imaging

sub-system.

The 3D line laser consists of three primary components, including the imaging

component, the distance-measuring component, and the data processing component. The

imaging component is used to capture the pavement texture data using external infrared

laser illumination and the spatial high-intensity camera. This component consists of two

separate laser sensors to cover a full-lane width. Each laser sensor includes a dedicated

infrared laser illumination and a high-intensity, area-scanning camera. The distance-

measuring component provides a data-capturing signal by using a DMI, which is user-

customizable. The data processing component computes the captured data into 3D range

results using a high-performance workstation. As shown in **Figure 2-3Error! Reference source not found.**, the two laser sensors are installed on each side of the roof at the back of the GTSV. The current sensor delivers a resolution of 5 mm in the longitudinal direction and 1 mm in the transversal direction, with a resolution of 0.5 mm in the vertical direction. The field of view of the two sensors covers a full-lane width, i.e. 4 m. The research team configured both sensors at approximately 15 degrees clockwise to the transverse direction to avoid overlooking transverse cracks in the pavement. During data collection, each laser sensor uses a high-powered laser line projector with a customized filter to generate a fine infrared laser line illumining a strip of the pavement. The corresponding spatial high-intensity camera captures the deformed laser line on the pavement. From the captured image, range measurements are extracted (Tsai & Wang, 2013)**.** Error! Reference source not found. illustrates the collected data using the 3D line laser sub-system.
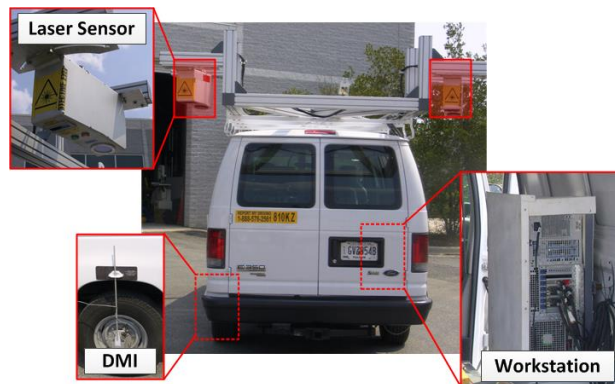
Figure 2-3. Photo. Components of 3D Line Laser System Integrated on the GTSV.

Figure 2-4. Photo. Collected data using the 3D line laser sub-system.

INTERSTATE HIGHWAY SYSTEM IN GEORGIA

The interstate highway system in Georgia is comprised of seven primary interstate highways, including Interstate 75 (Route No: 0401), Interstate 20 (Route No: 0402), Interstate 85 (Route No: 0403), Interstate 16 (Route No: 0404), Interstate 95 (Route No: 0405), Interstate 59 (Route No: 0406), and Interstate 24 (Route No: 0409), and eight auxiliary interstate, including Interstate 285 (Route No: 0407), Interstate 475 (Route No: 0408), Interstate 185 (Route No: 0411), Interstate 675 (Route No: 0413), Interstate 520 (Route No: 0415), Interstate 575 (Route No: 0417), Interstate 985 (Route No: 0419), and Interstate 516 (Route No: 0421). The total survey length of the interstate highway in Georgia covers 2,541.4 miles. **Figure 2-5** shows the spatial locations and extents of these interstate highways.
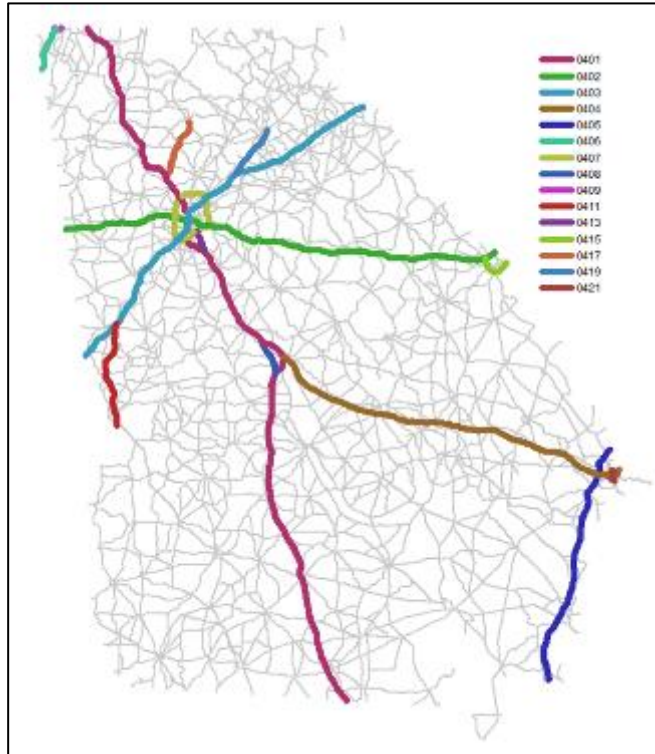
Figure 2-5. Map. Spatial locations and extents of the interstates in Georgia.

CHAPTER 3. SIGN INVENTORY BASED ON PREVIOUSLY COLLECTED DATA

This chapter presents a procedure to create an updated sign inventory for Georgia's interstate highway in 2018 using the sign inventory previously created in 2015 (RP 15-11). The key steps involved in this procedure include 1) collecting and preparing the video log images and their GPS locations, 2) matching signs in the 2015 sign inventory to the 2018 video log to validate the existence of the signs and verifying their conditions (good, surface failure, post failure, or obstruction), and 3) performing QA/QC operation to capture the unmatched signs from the 2015 sign inventory and the newly installed signs after 2015. Following the above procedure, this chapter discusses the results of the newly generated 2018 sign inventory, including the distribution of signs on each interstate highway and GDOT working district, grouped by the sign classification (regulatory, warning, guide and other signs), sign condition and sign overhead type (ground, sign bridge, bridge mounted, cantilever, and butterfly). Finally, this chapter also compares the 2015 sign inventory and the 2018 sign inventory in terms of the number of signs in different classifications and conditions.

KEY CHARACTERISTICS OF TRAFFIC SIGNS

This section defines the main traffic sign characteristics that were collected and extracted using the GTSV, including the inventory and condition assessment. Inventory describes the sign locations and their attributes (e.g. classification of traffic signs), while condition assessment describes the performance adequacy of the inventoried signs, such as surface

failure, post failure, obstruction, or in good condition. The location, classification, and conditions of the signs are identified as the key characteristics that are required for the inventory.

Sign Location: Traffic sign location is defined by GPS coordinates (i.e., longitude and latitude) that can uniquely define the spatial position. Extracting the location for each individual sign is the most important step for traffic sign inventory. In this study, WGS84, geodetic GPS coordinates are used to represent the traffic sign location, which can be flexibly converted to a linear referencing system that is used in GDOT.

Sign Classification: Traffic sign classification is defined as the traffic sign classes that can distinguish different traffic sign functionalities, which has led to different designs, e.g. RX-X as regulatory signs, WX-X as warning signs, etc. (note: X is a number.). There are more than 670 types of traffic signs defined in the MUTCD, and they belong to three functional classifications (McGee, 2010): regulatory, warning, and guide. These 670 sign types are used in this project. **Figure 3-1** shows an example of the different sign classifications used in this project.

A. Subfigure of regulatory sign   B. Subfigure of warning sign

C. Subfigure of regulatory sign

Figure 3-1. Photos. Examples of sign classification.

In addition, there could be some sign types that only occur within certain states or regions and are assigned with internal MUTCD codes. These signs will be classified and assigned to regulatory, warning, or guide classification based on their function. For example, the white sign "Prohibited. Holding Mobile Devices While Driving" is used in Georgia and will be classified as regulatory. All other signs that do not fall under any of these functional classifications, such as temporary work zone signs, information signs with no MUTCD code, etc., will be classified as "other" in this project.

Sign Condition: Traffic sign condition is represented by visual defects and the retroreflectivity. In this study, daytime inspection using video log images is the focus that identifies visual defects; studying the retroreflectivity condition, which is covered by nighttime inspection, is not presented in this chapter. Four categories of poor sign conditions are defined in this study, including post failure, dirty, obstruction, and surface failure. **Figure 3-2Error! Reference source not found.** shows several examples of signs in poor condition in each category.

A. Subfigure of surface failure   B. Subfigure of post failure

C. Subfigure of dirty sign   D. Subfigure of obstructed sign

Figure 3-2. Photos. Examples of four categories of poor sign conditions.

Based on the Signs Chapter of GDOT's Foreman's Academy (2008), the four categories of poor sign conditions correspond to four maintenance actions defined by the Highway Maintenance Management System (HMMS) (Hensing & Rowshan, 2005), including straightening, cleaning, vegetation trimming, and replacing.

Overhead Sign: Besides the above-mentioned three traffic sign characteristics, overhead signs are specially considered and separated from ground-mounted traffic signs. Although overhead signs only contribute a small portion of the entire sign population, the damage of these signs and/or their corresponding support, e.g. panel failure, support structure failure, etc., may potentially lead to serious hazards to road users. **Figure 3-3** shows an example of such hazardous situations.

Figure 3-3. Photo. Example of overhead sign failure (FHWA, 2013).

Therefore, overhead signs are specially categorized and inventoried in detail. According to the different supporting structures for overhead signs defined in the Signs Chapter of GDOT's Foreman's Academy (2008), four categories are inventoried, including Sign-Bridge-Mounted, Cantilever-Mounted, and Bridge-Mounted and Butterfly-Mounted traffic signs. **Figure 3-4** illustrates these four categories. Inventorying the detailed categories of overhead signs and identifying the spatial locations of these signs will be beneficial to the subsequent maintenance and/or the more detailed structural inspection.

A. Subfigure of sign-bridge-mounted

B. Subfigure of cantilever-mounted

C. Subfigure of bridge-mounted

D. Subfigure of butterfly-mounted

Figure 3-4. Photos. Examples of the overhead sign categories defined by GDOT.

PROCEDURE TO CREATE UPDATED SIGN INVENTORY USING PREVIOUSLY COLLECTED DATA

This section discusses the procedure adopted to create an updated sign inventory for Georgia's interstate highways based on the previously created sign inventory in 2015. The three key steps involved in this procedure include 1) collecting and preparing the interstate video log images and their GPS locations, 2) matching signs in the 2015 sign inventory to the 2018 video log to validate its existence and assessing the sign condition (good, surface failure, post failure, or obstruction), and 3) performing QA/QC operation to capture the unmatched signs from the 2015 sign inventory and to capture the newly installed signs since 2015. **Figure 3-5** shows the flowchart of the proposed procedure, which consists of the 3 key steps.
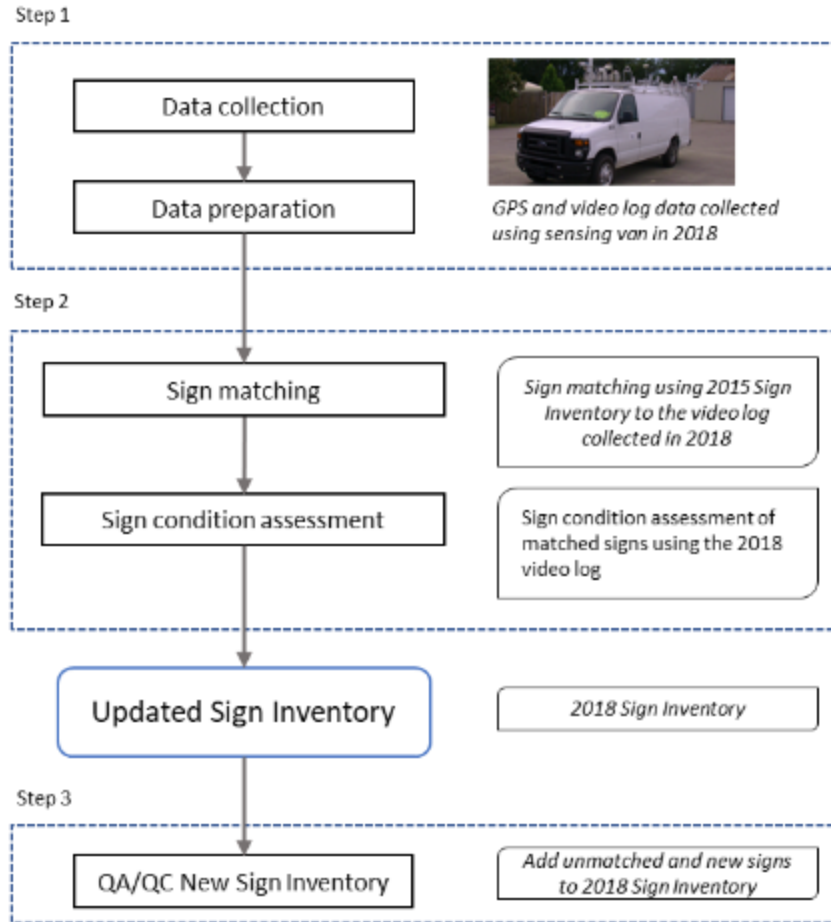
Figure 3-5. Flowchart. Procedure to create an updated sign inventory using the previously collected data.

RESULTS

In this study, 21,427 traffic signs are inventoried through the proposed approach. Among all the identified signs, the majority of the signs are guide signs that make up 65% of the total population (13,969 signs). The rest of the population consists of 4,465 regulatory signs, 2,717 warning signs, and 276 other signs (temporary signs and signs without identifiable MUTCD codes). **Figure 3-6** shows the distribution and the percentage of the traffic signs on the interstate highways in Georgia based on their classifications. **Error!**

Reference source not found.Table 3-1 lists the number of signs in each category on each interstate highway.

Traffic Sign Classifications on Interstate Highways in Georgia

276 1%
4465 21%
2717 13%
13969 65%

■ Regulatory Signs ■ Warning Signs ■ Guide Signs ■ Other Signs
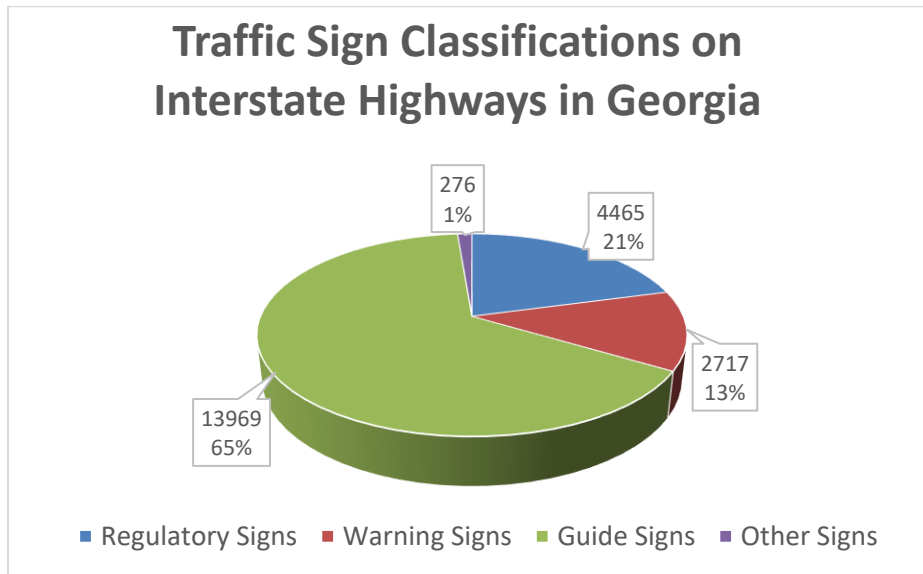
Figure 3-6. Chart. Distribution of traffic sign classifications on interstate highways in Georgia.

Table 3-1. Detailed statistics of traffic signs MUTCD categories

Interstate	Guide Signs	Regulatory Signs	Warning Signs	Other Signs	Total
I-16	1,423	381	230	22	2,056
I-185	446	88	76	2	612
I-20	2,289	720	294	44	3,347
I-24	50	20	20	0	90
I-285	1,478	364	214	23	2,079
I-475	130	42	20	0	192
I-516	126	54	80	0	260
I-520	176	55	81	3	315
I-575	411	104	142	15	672
I-59	129	61	35	1	226
I-675	76	31	21	0	128
I-75	4,026	1,561	942	75	6,604
I-85	2,016	619	264	64	2,963
I-95	870	292	254	21	1,437

| I-985 | 323 | 73 | 44 | 6 | 446 |

Among all the identified signs, 6% of the signs (i.e. 1,256 signs) are in different categories of poor condition as defined in the GDOT's Foreman's Academy (2008). Among all the signs in different poor condition categories, surface failure (478 signs, 38.1%) and dirty signs (302 signs, 24.0%) are the two primary categories of poor conditions. The rest of the signs are in poor condition due to having a failed post (199 signs, 15.8%) and being obstructed (277 signs, 22.1%). Overall, the number of traffic signs in poor condition is only a small portion of the total number of traffic signs, indicating overall, well-maintained sign condition by GDOT. **Figure** 3-7 and **Figure** 3-8 show the distribution of the traffic signs in poor condition on the interstates. **Table 3-2** shows the detailed statistics for each interstate highway in Georgia that are in poor condition.
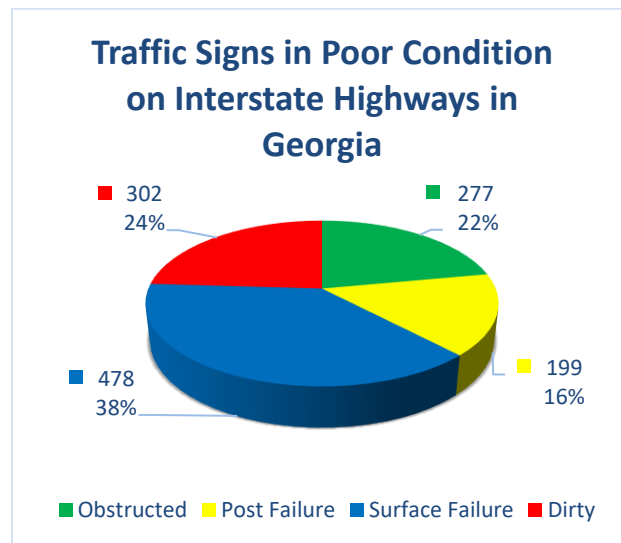
Figure 3-7. Chart. Traffic signs with poor conditions on interstate highways in Georgia.
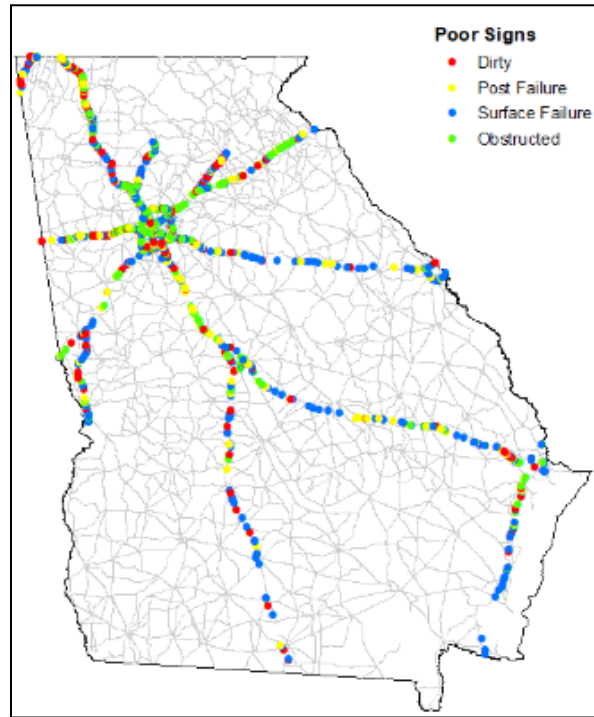
Figure 3-8. Map. Traffic signs with poor conditions on interstate highways in Georgia.

Table 3-2. Detailed statistics of traffic signs in poor conditions on each interstate highway.

Interstate	Obstructed	Post Failure	Surface Failure	Dirty	Total
I-16	18	22	41	20	101
I-185	7	3	22	11	43
I-20	45	35	72	34	186
I-24	1	3	2	8	14
I-285	59	19	56	22	156
I-475	2	1	5	5	13
I-516	0	0	5	0	5
I-520	0	2	9	0	11
I-575	4	5	23	18	50
I-59	0	3	8	9	20
I-675	1	1	2	7	11
I-75	80	78	136	101	395
I-85	51	15	44	21	131
I-95	9	2	29	11	51
I-985	0	10	24	35	69

Among all the inventoried signs, 19.3% of the signs (i.e. 4,135 signs) are installed on overhead structures (sign-bridge, cantilever, bridge and butterfly signs). About 42% of the overhead signs (i.e., 1,733 signs) are installed on sign-bridges, while 35.2% of the overhead signs are installed on bridges or other permanent overhead structures (i.e., 1,457 signs). The rest of the overhead signs are installed either on cantilever structures (10.1%, 417 signs) or butterfly structures (12.8%, 528 signs). **Figure 3-9** and **Figure 3-10** show the distribution of the overhead signs on the interstate highways in Georgia based on their base supporting structures.
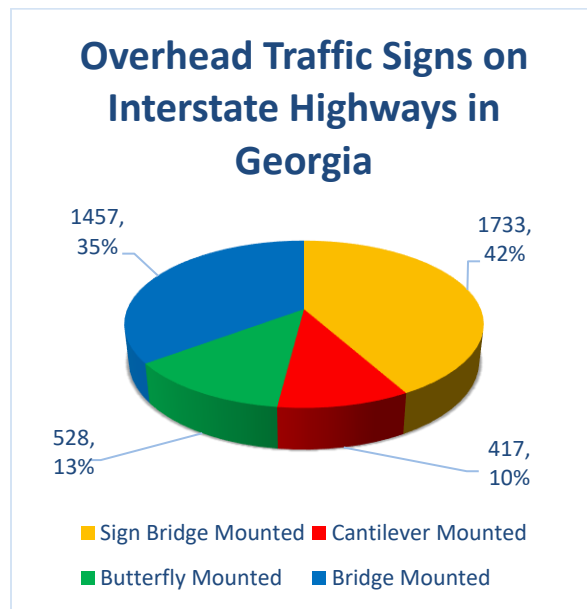
Figure 3-9. Chart. Overhead traffic sings on interstate highways in Georgia.
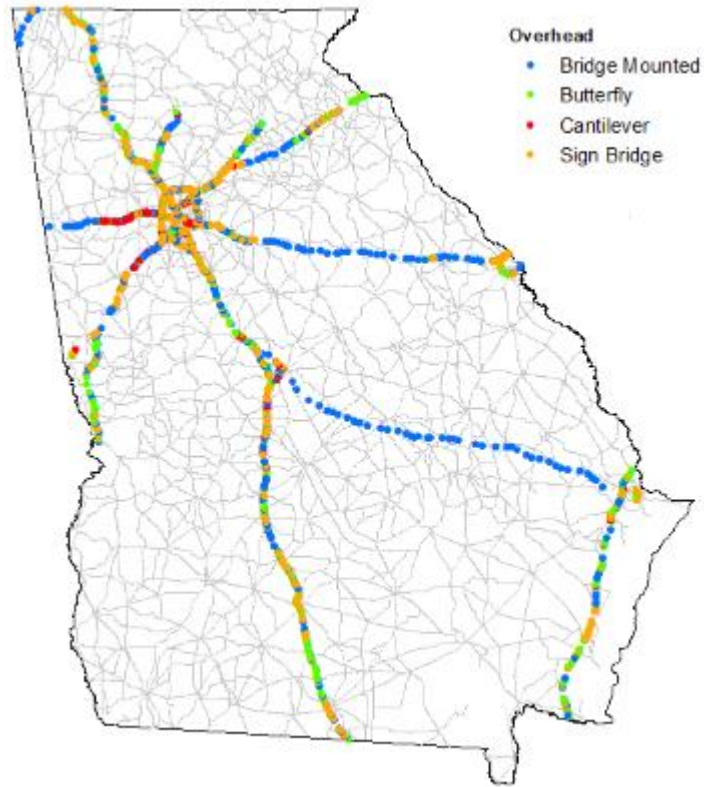
Figure 3-10. Map. Overhead traffic sings on interstate highways in Georgia.

Traffic signs installed on overhead structure on interstate highways in Georgia. **Table 3-3** shows the detailed statistics for each interstate highway in Georgia.

Table 3-3. Detailed statistics of overhead traffic signs on each interstate highway.

Interstate	Sign Bridge Mounted	Cantilever Mounted	Butterfly Mounted	Bridge Mounted
I-16	19	0	1	81
I-185	35	6	12	45
I-20	254	89	70	301
I-24	11	0	0	2
I-285	274	31	45	187
I-475	15	0	14	12
I-516	10	0	0	1
I-520	34	4	3	14
I-575	25	2	2	38

I-59	4	0	0	9
I-675	11	3	1	14
I-75	575	167	266	485
I-85	371	75	51	183
I-95	82	39	43	67
I-985	13	1	20	18
Total	1733	417	528	1457

Among all the working districts, District 7 has most of the traffic signs, approximately

28% (i.e., 5,989 signs) of the total interstate traffic signs, because the district covers the

majority of the urban interstate highways. District 4 covers the least number of the traffic

signs, approximately 7.5% (i.e., 1,606 signs) of the total interstate traffic signs because of

short mileage the interstate covers in this district. **Figure 3-11** and **Figure 3-12** show the

distribution of the interstate miles in the seven districts and the corresponding numbers of

traffic signs within each district.

Table 3-4 shows the detailed numbers and percentage of traffic signs in each working
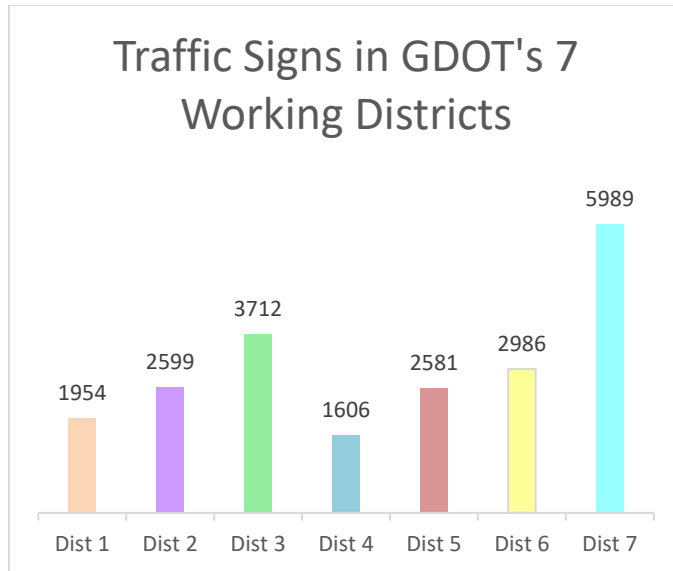
district.

Figure 3-11. Chart. Distribution of the interstate traffic signs in the 7 working districts.
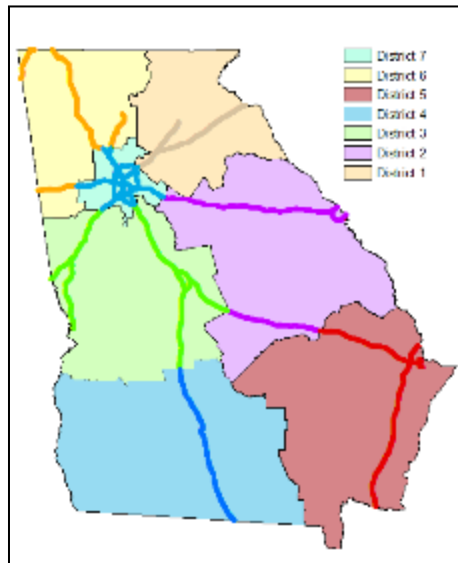
Figure 3-12. Map. Distribution of the interstate traffic signs in the 7 working districts.

Table 3-4. Detailed numbers of traffic signs in each working district.

District	1	2	3	4	5	6	7	Total
Number of Signs	1954	2599	3712	1606	2581	2986	5989	21427
Percentage	9.1%	12.1%	17.3%	7.5%	12.0%	13.9%	28.0%	100.0%

The distribution of the traffic signs in poor condition in the seven working districts is shown in **Figure 3-13**. It can be observed that District 7 has more traffic signs in poor conditions (i.e., 462 signs, approximately 8% of the total signs in District 7) than the ones in other districts. While surface failure is the major reason in all working districts for traffic signs in poor condition, it should be noticed that traffic signs with dirty surfaces occur more frequently in District 6, and obstruction and post failure occur more frequently in District 7. These observations may provide some insight into guiding an improved maintenance effort, such as traffic sign cleaning in District 6, and repair the sign posts and vegetation trimming in District 7.
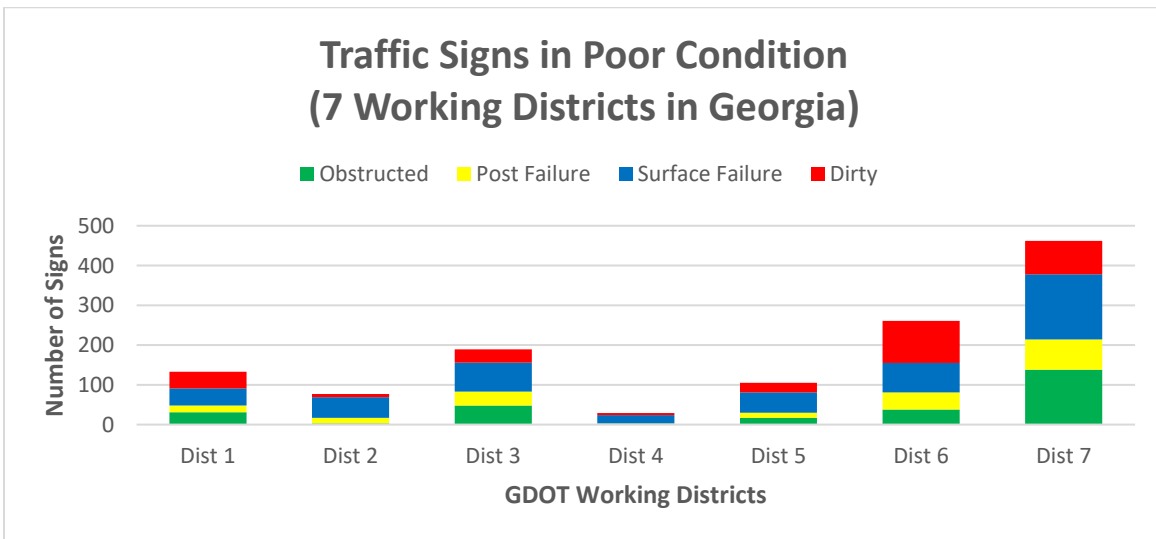
Figure 3-13. Chart. Distribution of traffic signs in poor condition in the 7 working districts.

Table 3-5 shows the detailed statistics including the count of different types of poor

condition signs and the percentage of poor condition signs in each district.

Table 3-5. Detailed statistics of traffic signs in poor conditions in each working district.

District	Obstructed	Post Failure	Surface Failure	Dirty	Total	Percent Poor Condition
1	31	17	43	42	133	7%
2	3	14	52	8	77	3%
3	48	35	73	33	189	5%
4	2	1	21	5	29	2%
5	17	13	51	24	105	4%
6	38	43	74	106	261	9%
7	138	76	164	84	462	8%

Figure 3-14 shows the distribution of the overhead traffic signs in the 7 working districts.

It can be observed that District 7 has a significantly larger number of overhead traffic

signs (i.e., 1,954 signs, around 33% of the total signs in District 7) than other districts

because of the frequent overpasses and intersections in the urban region. The large

number and percentage of overhead signs in District 7 may require more maintenance

efforts and activities than in other districts. Table 3-6 shows the detailed statistics of the

overhead traffic sign distribution and the percentage of overhead signs in each district.
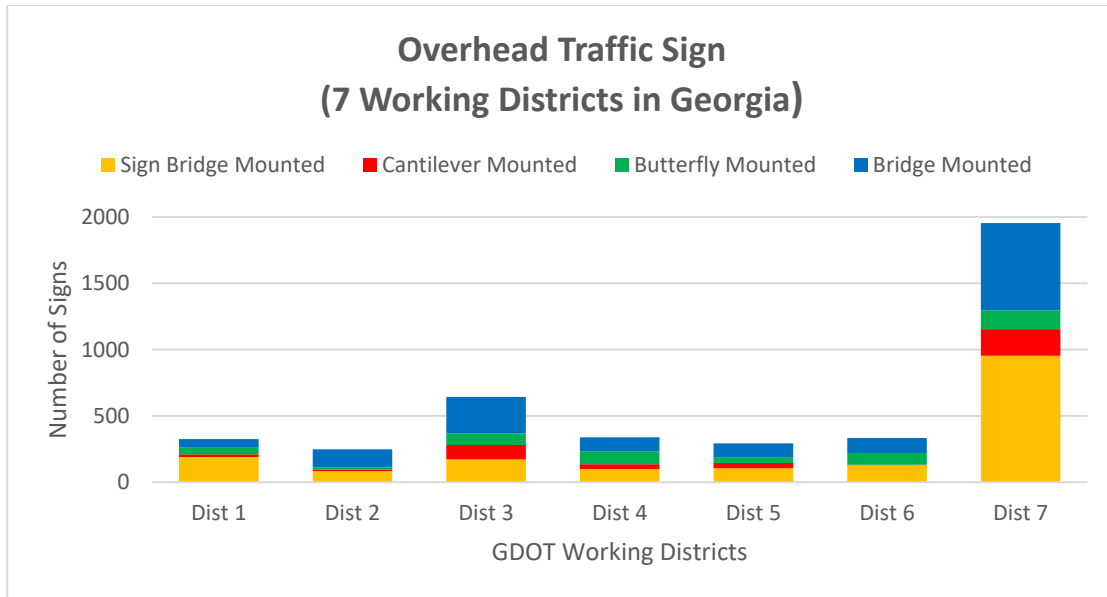
Figure 3-14. Chart. Distribution of the overhead traffic signs in the 7 working districts.

Table 3-6. Detailed statistics of overhead traffic signs in each working district.

District	Sign Bridge Mounted	Cantilever Mounted	Butterfly Mounted	Bridge Mounted	Total	Percent Overhead Signs
1	190	20	50	65	325	17%
2	84	9	18	137	248	10%
3	172	108	87	276	643	17%
4	99	37	98	104	338	21%
5	106	39	44	104	293	11%
6	128	4	88	114	334	11%
7	954	200	143	657	1954	33%

COMPARISON OF 2015 AND 2017 SIGN INVENTORY

This section presents the statewide comparison of the changes in the number of signs in different sign classification and sign condition between the 2015 and 2018 sign inventories. For the sign classification comparison, only the regulatory, warning, and guide signs are compared.

First, the comparison is between the number of signs in different sign classifications. A total of 21,151 signs were inventoried in 2018 that belonged to the regulatory, warning, and guide classification, compared to 20,763 signs that were found in the respective classes of the 2015 sign inventory. Overall, it is an increase of 1.87%, a small number compared to the total number of signs. **Table 3-7** shows the comparison of the number of signs in each class between the 2015 and 2018 sign inventories. Most sign changes were in the "regulatory" sign category, which accounted for a 4.4% increase in the number of signs in 2018. For example, in the recent times, Georgia made it illegal to hold mobile devices while driving, and a new regulatory sign was introduced in Georgia after 2015. This example justifies the increase in the number of regulatory signs in 2018. There is also a small increase (1.5%) in the number of guide class signs. One reasoning to this increase is that the signs along I-516 in the northbound direction were not included in the 2015 sign inventory. In addition, there is a small percentage decrease in the number of signs in warning sign class, which are 0.55 percent. Some of the reduction can be part of sign removal for the construction work such as the construction of new interchange near Macon.

Table 3-7. Comparison of the number of signs in different sign classification between 2015 and 2018 sign inventory.

Sign classification	2015	2018	Percent change
Regulatory Signs	4,277	4,465	4.4%
Warning Signs	2,732	2,717	-0.55%
Guide Signs	13,754	13,969	1.5%

Among the signs inventoried in 2018, 1,256 signs are in poor condition but only 897 signs were in poor condition in 2015. **Table 3-8** shows the comparison of different categories of poor condition signs between 2018 and 2015. There is a 40% increase in the number of signs in all categories of poor condition in 2018 compared to 2015. There are more obstructed signs (129%, the highest increase); the number of signs in the dirty category has the lowest increase (over 15%). There is a 23% increase in the signs with surface failure and a 62% increase in the signs with post failures. In the 3 years between the inventories, it is possible some of the poor condition signs were not repaired and additional signs dropped into poor condition. It must be noted that the individual signs were not tracked for the condition change and the results are only an aggregated count from the entire state. Therefore, detailed studies are required to confirm the actual reason for the increase of signs in poor condition.

Table 3-8. Comaprison of the number of signs in different poor condition categories between 2015 and 2018 sign inventory.

	2015	2018	Percent change
Obstructed	121	277	129%
Post Failure	123	199	62%
Surface Failure	390	478	23%
Dirty	263	302	15%
Total	897	1256	40%

SUMMARY

The following is a summary of the sign inventory in this project:

- **21,427** traffic signs were inventoried in 2018 along all the interstate highways in Georgia using a procedure that makes use of previously collected data (2015 sign inventory). The guide signs make up 65% (13,969 signs) of the total sign population on the interstate. The rest of the population consists of 4,465 regulatory signs, 2717 warning signs, and 276 other signs (temporary signs and signs with no identifiable MUTCD code).

- There are **1,256** signs (6% of the overall traffic sign population) in poor condition that require sign maintenance, including the following:

  1) Surface failure (478 signs, 38 %)

  2) Dirty (302 signs, 24%)

  3) Post failure (199 signs, 16%)

  4) Obstructed (277 signs, 22%)

- There are **4,135** overhead signs (19% of the overall traffic sign population). They have a high potential risk and require frequent monitoring and condition assessment. They are divided into four categories and inventoried with their locations (latitude and longitude coordinates).

  1) sign-bridge (1,733 signs, 42%)

  2) bridge-mounted (1,457 signs, 35%)

  3) cantilever (417 signs 10%)

  4) butterfly (528 signs, 13%)

- There is an increase of 1.87% in the number of signs in the 2018 Sign Inventory compared to the 2015 Sign Inventory. For example, regulatory signs such as the "Prohibited. Holding Mobile Devices While Driving" signs were installed after 2015 when the state of Georgia passed the Hands Free Georgia Law (HB673) contributed to this increase.

- There is a 40% increase in the number of signs in poor condition in the 2018 Sign Inventory compared to the 2015 Sign Inventory. Further studies are needed to determine the number of poor condition signs in 2015 that were not repaired until 2018 and to determine the number of additional signs that dropped into poor condition.

CHAPTER 4.   SIGN RETRO-REFLECTIVITY CONDITION ASSESSMENT USING MOBILE LIDAR

This chapter presents a sign retro-reflectivity condition assessment method using LiDAR technology, validates the proposed method, and uses a case study to demonstrate the use of the proposed method. The proposed method aims to cost-effectively classify the sign retro-reflectivity condition at network-level based on good, poor, and uncertain categories. After the sign retro-reflectivity condition is determined by the proposed method at the network-level, GDOT inspectors may only need to screen and assess the signs that are in poor and uncertain categories to recommend suitable actions (e.g. replace sign, wash, etc.). Therefore, the proposed method not only complements GDOT's existing sign retro-reflectivity condition assessment methods (e.g. time-consuming nighttime visual inspection and retroreflectometer measurement methods), it will enormously cut down GDOT's sign inspection efforts at the network-level by focusing on signs that need the most attention (poor or uncertain category signs). This chapter also presents the retro-reflectivity change analysis for four years of selected signs to track their retroreflectivity deterioration behavior. Promising trends can be observed in terms of retroreflectivity deterioration behavior by analyzing the retro-intensity change on the signs. However, dirt accumulation on the signs over time can affect the retroreflectivity measurement and, in turn, affect the conclusions we can draw about the deterioration status. So, it is recommended to clean the sign first before condition assessment so as to have a consistent measurement for deterioration analysis.

INTRODUCTION

Although only 20% of driving occurs after dark, there are three times more deaths at night than during the day (Brody 2007). Drivers at night rely on the visibility of traffic control devices (TCD), such as traffic signs and pavement markings, for navigation and maintaining their driving lanes. However, if the crucial navigation information from the TCDs cannot be seen by the drivers due to poor visibility at nighttime, it creates dangerous situations that often lead to crashes. Hence, for adequate visibility of the TCDs at night, ensuring the retro-reflectivity condition of signs and pavement markings above the minimum retro-reflectivity requirement is a priority for state departments of transportation. There are two current methods being used to assess individual traffic signs' condition to ensure their retro-reflectivity conditions are above the minimum MUTCD requirement (FHWA, 2012): the nighttime visual inspection, the retro-reflectometer measurement (Carson & Lupes, 2007). The nighttime visual inspection suffers from subjective assessment of the inspectors and lacks any objective standards, while the retro-reflectometer method is time-consuming, dangerous, and only samples 4 points, despite having the advantage of being able to provide objective, numerical data. Alternatively, transportation agencies may adopt blanket replacement methods to avoid individual sign retro-reflectivity condition assessment. However, this method may not result in economical use of resources because the signs in good condition are also replaced with this method. The three methods are described in detail in the following section.

CURRENT PRACTICES TO MEET THE MINIMUM RETRO-REFLECTIVITY REQUIREMENT FOR THE TRAFFIC SIGNS

This section discusses the two principle methods for traffic sign retro-reflectivity condition assessment and is followed by a discussion on the blanket replacement method.

Method 1: Nighttime visual inspection method

According to FHWA guidelines (FHWA, 2007), visual night-time inspection is an assessment method in which two trained inspectors travel in a truck or SUV at a normal driving speed using low-beam headlights. The passenger-inspector gives an evaluation ("acceptable" or "unacceptable") to each sign being surveyed. The greatest disadvantage with this method is its subjectivity. The process depends entirely on human judgement, which cannot be quantified and may vary from person to person.

To counter that, state agencies standardize the assessment procedure by including a "calibration" phase before the inspection during which several traffic signs known to be in a passing/failing condition are used as references to train the inspectors (FHWA, 2007; MnDOT, 2014). However, even such standardization may not account for variability in assessment under different environmental conditions (like surrounding light, fog, etc.) that may be faced during actual field assessment. An additional issue with the visual inspection procedure is that it   is only useful if done at night.

In GDOT sign condition assessment practices, GDOT does not have a separate sign retroreflectivity condition assessment procedure. Their retro-reflectivity condition assessment is tied up with overall sign condition assessment, which includes evaluation

of fading, cracking, adhesion failure, post failure, bolt failure, and post galvanization (GDOT, 2012). The Georgia Tech research team interviewed a GDOT inspector from District 7 to document the standard operating procedure for GDOT inspectors to assess traffic signs. GDOT typically assesses the retro-reflectivity conditions of the signs in their area once every year. To perform the assessment, GDOT sign inspectors typically drive their trucks to a distance of 300-450 feet in front of the sign to start with the retro-reflectivity condition assessment. The inspector turns ON the flashing amber light and the headlights of his truck to check if he can clearly see flashes reflected from the traffic sign. This is done to check the reflectivity of the background color of the sign. Once it is done, flashing lights are turned OFF, and with the help of just the truck's headlights, the inspector verifies whether the legend on the sign is visible or not. If both the above conditions are satisfied, the sign passes the retro-reflectivity test. Following the retro-reflectivity assessment, the inspector also looks at other failures (cracking, post failure, etc.) to determine the overall condition of the sign.

There are four main limitations of GDOT's sign retro reflectivity condition assessment: 1) it is time-consuming to stop and assess every sign; 2) there are thousands of signs in the network, so it takes many months to complete the assessment; 3) inspectors can conduct the inspection only at nighttime, so they have only limited time to conduct their assessment; and 4) the subjectivity involved in retroreflectivity assessment (how much reflectivity is good) means that different inspectors from different districts may have different assessments of the signs; therefore, assessment results may not be uniform across the state.

Method 2: Retroreflectometer method

The second method uses a retroreflectometer, which is a handheld device that is held directly against the surface of a sign at 4 different points on each color of the sign to measure the retroreflectivity value (ASTM, 2016). A numerical retroreflectivity value is given that can then be compared to the minimum levels outlined in the MUTCD (2009) to classify the sign as passing or failing. The method is quantitative and consistent, thereby overcoming the subjectivity of the visual assessment method. However, the primary issue with this method is that it is very slow, tedious (labor-intensive) and dangerous to workers making the measurement in the field. Inspectors must leave their vehicle for every measurement, which is time-consuming (approximately 5 minutes for each sign) and dangerous (while traffic is still flowing). Another concern is that this 4-sampling method does not work well when the sign condition is non-uniform. For example, **Figure 4-1** (a) and **Figure 4-1** (b) show two sets of 4-point readings, measured on the same sign (a STOP sign with dirt on right side and scratches on left top corner). **Figure 4-1** (a) shows the sampling location at which the sign is assessed as "Pass" and **Figure 4-1** (b) shows a sampling location at which the sign is assessed as "Fail" simply because four different points are selected. Thus, for signs with a non-uniform condition, the results of this assessment may fail to account for localized damage and deterioration.

A. Subfigure of pass sample   B. Subfigure of fail sample

Figure 4-1. Photos. Variation of retro-reflectivity assessment results for a non-uniform sign condition.

Method 3: Blanket replacement method

Blanket replacement is a method of TCD asset management to ensure the retro-reflectivity conditions of the signs are above the minimum MUTCD requirement. This method considers both the expected life of the sign and its location for a replacement decision. More specifically, a group of signs in a single area or corridor is set to be replaced all at once under the assumption that all signs in the group would have reached their expected life spans. This method is currently used by many state DOTs. Typically expected sign lives that are used for setting the replacement schedule are 7-10 years for engineering grade signs, 10-15 years for high-intensity prismatic signs, and 15 years for Type VI or higher prismatic signs (FHWA, 2007). These timeframes may also be adjusted based on climate and previous experience in the region. In addition, blanket replacements of signs may also be scheduled along a corridor during road construction work, regardless of their service life.

This method eliminates the need for field assessment, decreases the number of trips made to replace signs, and reduces the amount of documentation required, since the only necessary information is the last date of replacement for a sign group. The major disadvantage of the blanket replacement method is that signs in good condition may be prematurely replaced, even though they may still have several months or years of service remaining, which is an uneconomical use of agency resources. This risk becomes more likely in cases in which individual signs are prematurely replaced (due to theft, post failure, or vandalism) between replacement cycles. Then, it is possible for a new sign to be taken down and replaced.

Table 4-1 compares the characteristics of the existing methods in terms of strengths and limitations, including assessment quality, speed, safety, and assessment time.

Table 4-1. Strength and weaknesses of assessment methods.

Method	Assessment quality	Speed	Safety	Assessment time
Visual Inspection	X Subjective; not quantifiable	X Time-consuming; must individually assess each sign	✓ No need for humans to enter roadway, can assess from inside the vehicle	X Must be done at night
Retroreflectometer	X Few points; may miss localized damage	X Time-consuming and laborious; must measure each sign by hand	X Human must enter right-of-way to conduct assessment	✓ Any time of day is viable
Blanket Replacement	X May remove signs that still have remaining life	✓ No time spent on assessment	✓ No field assessment	(N/A)

There is an urgent need to develop an alternative method for assessment and replacement of traffic signs to meet the minimum retroreflectivity requirement that is objective, rapid, cost-effective, safe, and not constrained by limited assessment time.

A COST-EFFECTIVE MEANS TO ASSESS SIGN RETRO-RETROFLECTIVITY CONDITION

The current sign condition assessment methods, including nighttime visual inspection and retroreflectometer measurement, are labor-intensive, time-consuming, dangerous to workers, subjective because of human assessment or having only four subjective sampling points, limited in terms of productivity, and constrained by time (only at night). Since it is very slow to have inspectors drive and evaluate all the roadways with the nighttime visual inspection method or retroreflectometer method, the inspections are typically only done once per year, so damaged signs may stay up for quite a long time without being replaced. The blanket replacement method is simple; however, it is not an economical method because some signs may still be in a good condition and do not need to be replaced.

The LIDAR technology could be a very effective method that saves a significant amount of time and resources for the traffic sign assessment. While LIDAR technology can be used to extract roadway assets, including signs (Tsai & Ai, 2014) and pavement marking (Haiyan et al., 2015), sidewalk measurement (Tsai & Ai, 2016), super-elevation measurement (Tsai & Ai, 2013), sight distance assessment (Ma et al., 2019) at highway speed (100km/hr), it would be beneficial to use the already-collected LIDAR cloud data, which can also be used to assess sign retro-reflectivity (Ai & Tsai, 2016).

The LIDAR data can be collected during any time (day or night) and does not require workers to physically stop and get into and out of a vehicle to perform data collection. LIDAR can capture more than 4 sampling points (e.g. 20 – more than 100 depending on type of LIDAR systems), much more effective than a reflectometer's 4 points, as illustrated in **Figure 4-2** (b) and **Figure 4-2**(c). LIDAR data provide a complete representation of the sign (**Figure 4-2** (c) that is close to the human eye's ability to visually and accurately perceive reflectivity (as shown in **Figure 4-2** (a)); this is much better than the using just the four data points of a retroreflectometer measurement of each color (as shown in **Figure 4-2** (b)). Hence, LIDAR technology can provide more objective and reliable assessment of a sign's retroreflectivity than can the retroreflectometer method.

A. Subfigure of nighttime visual inspection   B. Subfigure of retroreflectometer method
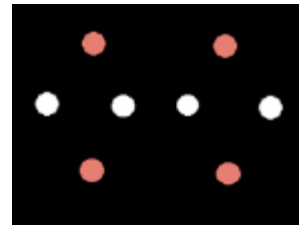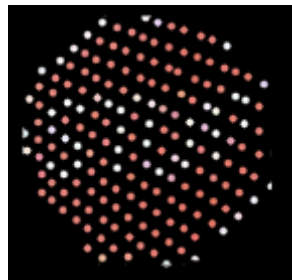
C. Subfigure of LIDAR method

Figure 4-2. Illustrations. STOP sign retro-reflectivity condition assessment methods.

LIDAR technology provides an innovative opportunity to perform cost-effective and safe assessment of the sign retro-reflectivity condition. However, there is still a need to develop and validate a method using LIDAR technology to assess the sign retro-reflectivity condition at the network level and when driving at highway speed. The following section presents the development of the proposed method.

DEVELOPMENT OF SIGN RETRO-REFLECTIVITY CONDITION ASSESSMENT USING MOBILE LIDAR

The idea in this section is to use the objectiveness of the retroreflectivity assessment and the comprehensiveness (assessing the sign completely, not using just 4 points) of the visual assessment to develop a method to classify sign retroreflectivity condition into three categories using the mobile LIDAR. The categories include "good," "poor," and "uncertain" retroreflectivity condition ratings. The good category signs do not require further inspection. The poor category signs definitely require replacement. The uncertain category signs require GDOT inspectors to further assess the sign to determine if it is good or poor. Both the uncertain and poor category signs require further investigation. The value of this project is that it can determine which signs are good signs so that GDOT can efficiently disperse its inspectors only to the poor and uncertain category signs, thus saving great amounts of money and resources that would otherwise be spent on inspecting the good category signs.

LIDAR mounted on a mobile vehicle can collect thousands of 3D data points from the roadway environment at roadway driving speed (100 km/hr). The data collected by the LIDAR system consists of a three-dimensional point cloud with each point defined by

three-dimensional coordinates (X, Y, and Z) and a retro intensity value. A retro-intensity value measures the ratio of the energy redirected from the object in the roadway environment to the energy emitted from the LIDAR sensor, similar to the measurement obtained when using a retroreflectometer (Ai, 2013). Hence, the retro-intensity values and the traffic sign retro-reflectivity conditions can be correlated. Such a correlation can be used to conduct a traffic sign retroreflectivity condition assessment. This section discusses the development of a novel sign retroreflectivity condition assessment method using the data collected by mobile LIDAR. This section does not discuss the data collection and data processing steps that includes (1) sensor calibration, (2) data acquisition, (3) LIDAR point coordinate computation, and (4) screening of the point cloud that is associated with traffic signs. These steps are described in the paper authored by Ai and Tsai (2014). After the 3D point cloud data for the traffic signs are screened, a sign retroreflectivity condition assessment includes three steps: 1) compute the retro-intensity statistics (such as median, 25th percentile) for the screened sign; 2) determine the suitable sign retro-intensity criteria to classify the sign retroreflectivity condition category (good, poor, uncertain) using the statistics; 3) map the signs with their retro-reflectivity condition categories (good, poor, and uncertain) on the road network. These three steps are described in detail below.

Compute the retro-intensity statistics for the screened signs

The screened data consists of the location information and the retro-intensity value of the 3D points belonging to the sign. The distribution of the retro-intensity of the points can potentially reveal useful information of the retro-reflectivity condition. Ai (2013) in his research stated that the median statistic of the retro-intensity values above the minimum

retroreflectivity MUTCD requirements (after correlating with retro-reflectivity) can be an adequate indicator to determine the overall condition of a traffic sign. In addition to a median, the sign retro-intensity statistics, such as percentiles, can be used with higher confidence to categorize the signs as good or poor. For example, if the 25th percentile of the sign's retro-intensity distribution (a value at which 75% of the retro-intensity is better than this value) is greater than a certain threshold, the sign can be classified as good.

Determine the suitable retro-intensity criteria to classify the sign retro-reflectivity condition category

In this step, the suitable statistics to classify the retroreflectivity condition are determined. First, the correlation between the retro-reflectivity measurement and the retro-intensity is established to determine the minimum retro-intensity (MR), a threshold value for minimum sign retro-intensity below which it does not meet the MUTCD requirement for retroreflectivity. Next, using the retro-intensity statistics and the MR, the criteria to classify the retroreflectivity condition as good, poor, or uncertain is determined.

Establish the correlation between the retro-reflectivity points and the retro-intensity points

In order to establish an accurate correlation between the retroreflectivity and retro-intensity, similar location LIDAR retro-intensity need to be measured. **Figure 4-3** shows an example of retro-reflectivity measurement and the corresponding retro-intensity measurement for establishing the correlation between the two values. In the first step, four-point measurements are made at four locations on the signs using the retroreflectometer per the standard procedure (ASTM E1709) in the four quadrants of the

sign. In the second step, the LIDAR retro-intensity points of the signs are projected to a

2D plane, and the retro-intensity points around (roughly 10 cm) the four retro-reflectivity

measurement locations are selected. For retro-intensity measurements made in each

location, the median retro-intensity value is computed.
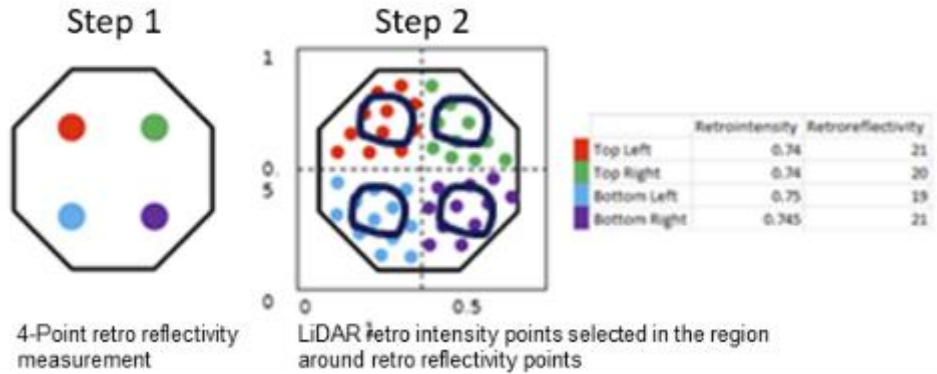
Figure 4-3. Illustration. Locations for retro-reflectivity.

Next, the retroreflectivity and corresponding median retro-intensity points are plotted to

establish a correlation and determine the MR, a threshold value for the minimum sign

retro-intensity below which the retroreflectivity is deemed to have failed the MUTCD

requirement. Good and poor condition signs were collected with the help of GDOT

engineers to establish the correlation between retro-reflectivity and the retro-intensity for

different colors and to determine the MR. Signs with prismatic sheeting type were chosen

for determining the MR because this sheeting type is predominately used on interstate

signs. The MUTCD specifies minimum requirements for retroreflectivity values for

yellow (50 cd/lx/m^2), green (15 cd/lx/m^2), and white (50 cd/lx/m^2) background-colored

signs. Therefore, the MR is determined for only green, yellow, and white signs. **Figure**

4-4, **Figure 4-5**, and **Figure 4-6** show the MR determination for green, yellow, and white

prismatic signs as 0.78, 0.76, and 0.76, respectively.
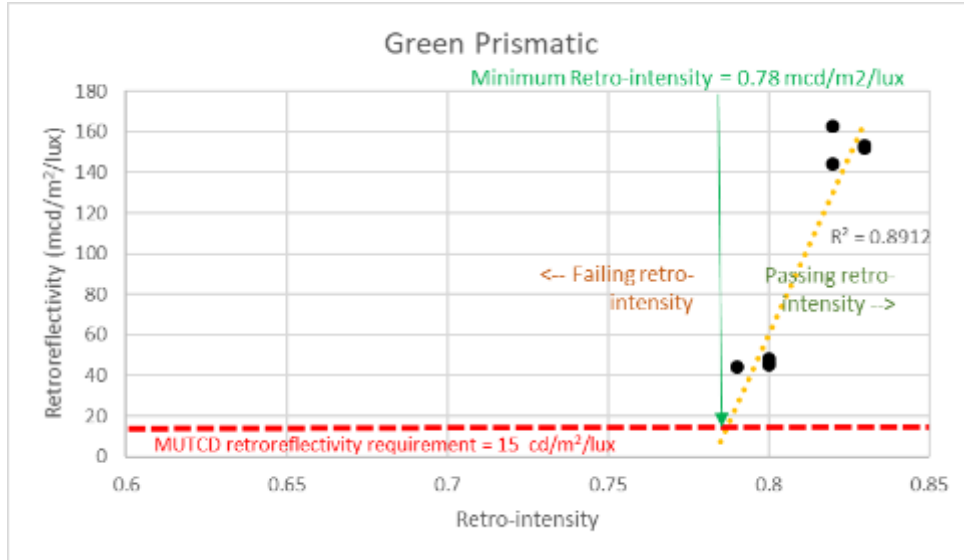
**Figure 4-4. Graph. Correlation between retro-reflectivity and retro-intensity and
determination of MR for green prismatic sheeting type signs.**
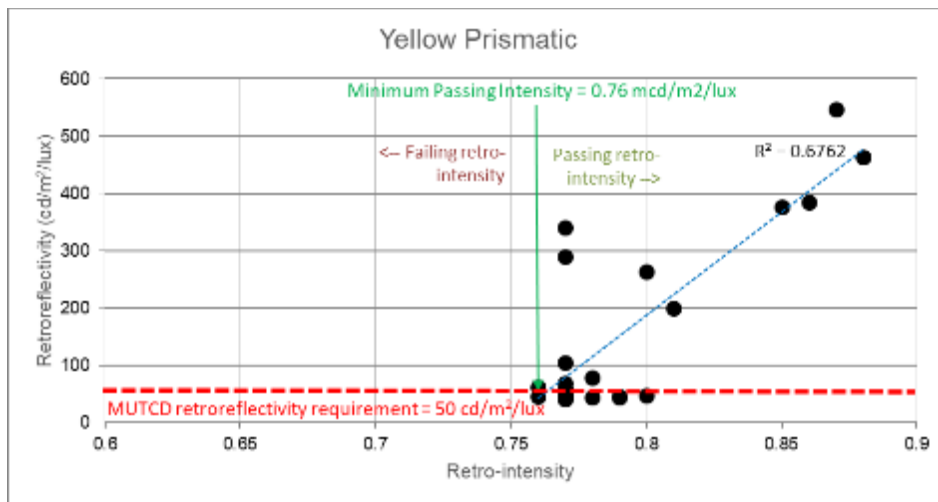
**Figure 4-5. Graph. Correlation between retro-reflectivity and retro-intensity and
determination of MR for yellow prismatic sheeting type signs.**
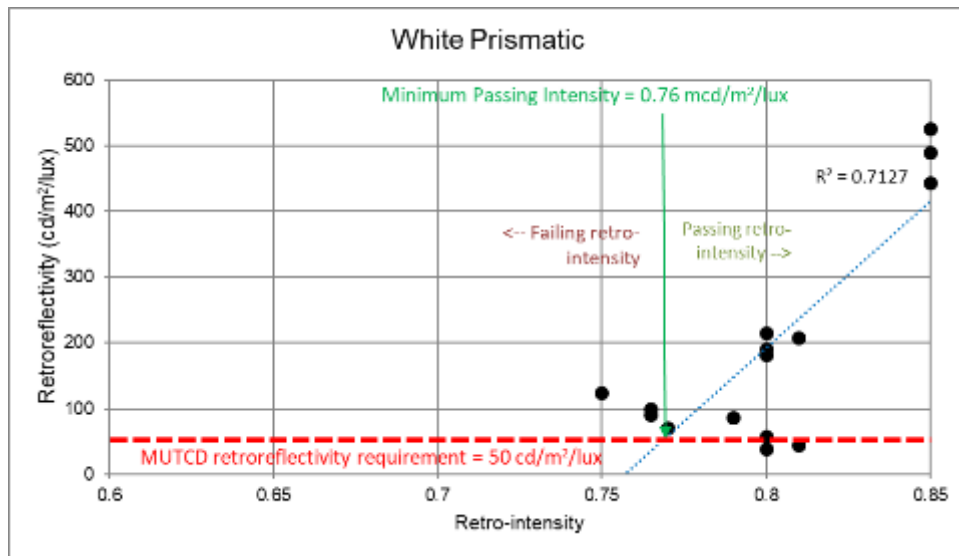
Figure 4-6. Graph. Correlation between retro-reflectivity and retro-intensity and determination of MR for white prismatic sheeting type signs.

Determine the criteria to classify the sign retroreflectivity category from the sign's retro-intensity values

The following are the proposed categories for classifying signs as good, poor, or uncertain.

○ Good category: The entirety or a majority of a sign's retro-intensity values are higher than MR. Quantitatively, the 25th percentile value is required to be larger than the MR. This ensures a high confidence when a sign is classified as good.

○ Poor category: A portion or the entirety of a sign's retro-intensity values are below MR. Quantitatively, the 50th percentile value (or median) is less than the MR.

○ Uncertain category: Quantitatively, the 25th percentile of a sign's retro-intensity is less than the MR and the median is greater than the MR.

Examples of the three categories described above are shown in **Table 4-2** using the MR (0.76) determined for yellow prismatic sheeting. For each color and sheeting type, the criteria would be the same, but only the MR value would be changed depending on the retroreflectivity and retro-intensity correlation, and the minimum MUTCD- required retroreflectivity.

Table 4-2. An example of sign retro-reflectivity condition classification using yellow prismatic sheeting signs with MR = 0.76.

Classification Criteria for yellow prismatic sheeting	Retro-reflectivity condition category
25th percentile retro-intensity > 0.76	Good
25th percentile retro-intensity < 0.76 < 50th percentile retro-intensity	Uncertain
50th percentile retro-intensity < 0.76	Poor

Map the signs with their retro-reflectivity condition category (good, poor, uncertain) on the road network

The third and the final step of the proposed method is to map the retroreflectivity condition of the signs by their condition category (good, poor, or uncertain) on the road network. This step is useful for locating the signs with different retroreflectivity conditions so that they can be screened and prioritized for further field assessment. Since the LIDAR technology collects the 3D points of the signs, the sign's location is obtained by computing the centroid of the 3D point cloud of the sign. The centroid value of the sign represents the location information (latitude, longitude, and altitude) and the

attribute information is represented by the sign's retroreflectivity condition category. The sign location and its retroreflectivity condition category are plotted on a map to visualize them on the road network.

VALIDATION OF SIGN RETRO-REFLECTIVITY CONDITION ASSESSMENT

The proposed method of assessing sign retroreflectivity condition category is developed based on the retroreflectometer measurements. However, GDOT conducts its sign assessment using the nighttime visual inspection method. Therefore, this section validates the proposed sign retroreflectivity condition assessment results with the GDOT inspector's assessment using same set of signs.

The Georgia Tech research team contacted the GDOT sign shop and District 7 Area office to collect the signs required to conduct the analysis. A total of 56 signs were collected, including different color and sheeting types. Among them, only 36 were of prismatic sheeting type. This is of interest to this research because the interstate signs are predominately of the prismatic sheeting type. Thirty signs in green, yellow, white, and blue backgrounds of prismatic sheeting type were collected.

An experiment was set-up to validate the proposed method by comparing the results with the nighttime visual inspection assessment. All the collected signs were assessed at Georgia Tech's campus on March 7, 2019, by the sign inspector from GDOT in the same manner as done normally for Georgia's state highway road signs. The test was performed 30 minutes after the sunset at 9.00 pm. A Georgia Tech parking lot was chosen for the visual assessment. The distance between the sign and the test vehicle was kept to

approximately 300 feet to replicate the real-world, night-time sign inspection method. The aerial view of the experiment set-up is shown in **Figure 4-7**. A tripod was set up at approximately 300 feet to hold the signs for the inspector to assess. After each assessment, the signs were replaced. The inspector assessed the signs and assigned "acceptable" or "unacceptable". Signs that that did not sufficiently reflect the headlight illumination or were dirty were put into the "unacceptable" category. Others were labeled as "acceptable" even when they were broken or had graffiti but still had high retro reflectivity.

Figure 4-7. Photo. The experimental setup created in Georgia Tech campus parking lot for GDOT inspector to assess the collected signs.

Figure 4-8 shows an example of a traffic sign (STOP) at the Georgia Tech campus and a test sign placed underneath it; these were assessed as unacceptable or acceptable by the GDOT inspector.

Figure 4-8. Photo. An example of poor (unacceptable) and good (acceptable) sign.

The retroreflectivity of all these signs was measured using a DELTA RetroSign retroreflectometer. The resulting R A values represent the retroreflectivity at an entrance angle of -4 degrees and an observation angle of 0.2 degrees. Four retro-reflectivity measurements were typically made for each sign, and the average value in $(cd/lx/m^2)$ was recorded. If there were more than one retroreflective color on a sign or if the legend was also retroreflective, four measurements of each color were taken and averaged. The average of the readings for each retroreflective color was compared with the MUTCD standard to determine the sign's retroreflective condition.

Finally, the Georgia Tech Sensing Van (GTSV), equipped with LIDAR, was used to collect the LIDAR data on the signs. Due to the limitation of acquiring the signs, only a limited number of signs were captured for assessment using LIDAR. The signs were

placed on tripods to hold them upright. The experimental set-up for the LIDAR data collection at the Georgia Tech campus for the yellow prismatic signs is shown in **Figure 4-9**. The signs were spaced approximately 10 meters apart and were placed at a 90-degree angle to travel direction to mimic the on-road condition. Four to 6 signs were set up in each round. The LIDAR data was collected from approximately, 10 m to the signs.

Figure 4-9. Photo. Experimental setup for sign LIDAR data collection at Georgia Tech campus.

Table 4-3 shows the number of prismatic signs in different colors that were tested using the retroreflectometer method, the visual inspection method, and the proposed method using LIDAR technology.

Table 4-3. Number of signs tested with different colors and methods.

Sign Color	Total number of signs	Retro-reflectivity method	Visual inspection method	Proposed LIDAR based method
White	8	8	8	5
Yellow	9	9	9	6
Green	7	7	7	3

The nighttime visual inspection results are used for validating the sign retroreflectivity condition assessment method developed in the previous section. The retroreflectometer readings were used to establish the correlation between the retroreflectivity and the retro-intensity value and to determine the MR for each color of the prismatic sheeting type. The developed criteria for the sign retroreflectivity condition classification was then validated with the visual inspection results. **Table 4-4** compares the visual inspection results and the sign retroreflectivity condition category obtained by the proposed method for the 14 signs (yellow, white, and green prismatic sheeting types).

Table 4-4. Comaprison of nighttime visual assessment result and the retro-reflectivity condition.

Sign No.	Color	GDOT inspector's retro-reflectivity assessment result	Retroreflectivity condition category by proposed method	Match
1	Yellow	Unacceptable	Poor	YES
2	Yellow	Unacceptable	Poor	YES
3	Yellow	Unacceptable	Poor	YES
4	Yellow	Acceptable	Good	YES
5	Yellow	Acceptable	Uncertain	NO
6	Yellow	Acceptable	Uncertain	NO
7	Green	Unacceptable	Poor	YES
8	Green	Acceptable	Good	YES
9	Green	Acceptable	Good	YES
10	White	Acceptable	Good	YES
11	White	Acceptable	Good	YES
12	White	Acceptable	Good	YES
13	White	Unacceptable	Poor	YES
14	White	Acceptable	Uncertain	NO

The developed method for categorizing the retroreflectivity condition using the mobile LIDAR shows promising results. From the 14 signs, 11 signs were correctly classified. All the signs that failed by the nighttime visual assessment method were correctly classified as "poor" by the developed method. Three signs (Nos. 5, 6, and 14) were

classified as "uncertain" by the proposed method despite being passed by visual inspection for retroreflectivity. The main reason for this classification is the presence of localized marks or cracks on the signs, which can result in gathering low retro-intensity values. shows the three signs that were categorized as uncertain by the proposed method. One can observe that the Sign No. 5 (as shown in **Figure 4-10** (a)) has graffiti at the bottom half and Sign No. 14 (as shown in **Figure 4-10** (b)) has mud spots on the right. Sign No.6 (as shown in **Figure 4-10** (c)) is classified as "uncertain" because there were many cracks on the sign, and the cracked part of the sign gives a low retro-intensity reading.

A. Subfigure of sign with graffiti   B. Subfigure of sign with mud spots

C. Subfigure of sign with cracked surface

Figure 4-10. Photos. Signs with uncertain retroreflectivity condition.

Based on the validation results, the proposed method is promising in categorizing the different retroreflectivity conditions. To ensure roadway safety, transportation agencies' priority should be to identify signs with poor retroreflectivity and replace them in a

timely manner. However, to review thousands of signs in their network is time-consuming. Therefore, the proposed method intends to confidently identify the good category signs so transportation agencies can only screen and focus their efforts on the remaining (smaller number) of poor and uncertain categorized signs in the network.

CASE STUDY

This section presents a case study to demonstrate the use of the proposed method using the traffic signs on the Interstate-285. The LIDAR data was acquired using right side LIDAR of the GTSV on August 8, 2018; therefore, 3D data was collected only from signs on the right side of the road. After data processing and screening, 338 signs were extracted and used for this case study. The proposed sign retroreflectivity condition assessment method was used to classify the 338 signs. Since the color for each sign was unknown, a lower MR value (0.75) was used in the proposed method for this demonstration. Sixty-seven signs were classified as "poor," 47 signs were classified as "uncertain" and the remaining 224 signs were classified as "good." **Figure 4-11** shows the map of the signs with different retro-reflectivity condition.
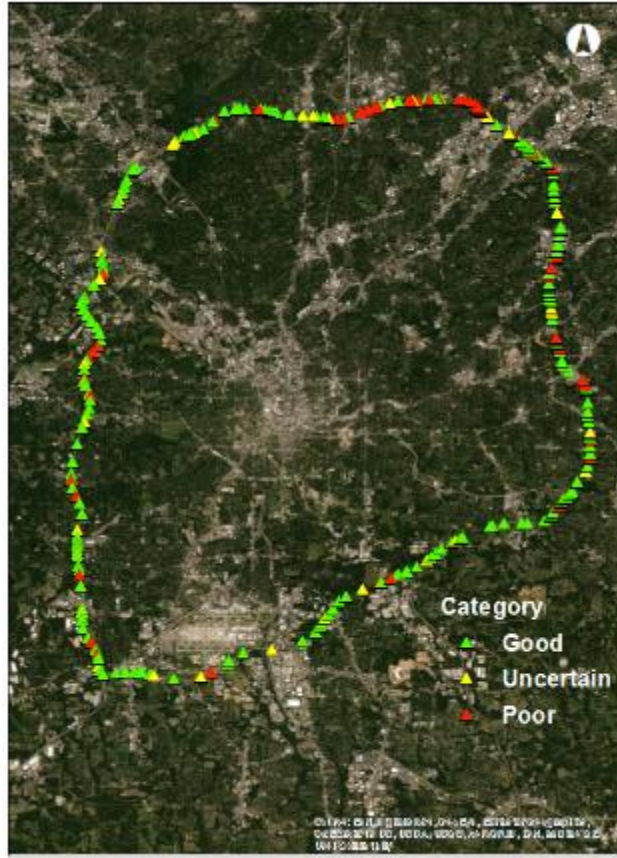
Figure 4-11. Map. Signs in good, uncertain, and poor retro-reflectivity condition on GA Interstate-285.

Figure 4-12 shows an example of some of the signs that were classified as poor. The typical concerns observed with the poor signs are that they are old, faded, or dirty (as seen in **Figure 4-12** (a), **Figure 4-12** (b), and **Figure 4-12** (c)). **Figure 4-12** (d) shows a sign that is clean and not faded; however, the sheeting type used does not appear to be prismatic sheeting type. This explains the poor classification of the sign, since the retro-reflectivity of this sheeting type falls under the "poor" category criteria set by the proposed method.

A. Subfigure of example 1   B. Subfigure of example 2

C. Subfigure of example 3   D. Subfigure of example 4

Figure 4-12. Photos. Example of signs in poor condition.

Sixty-seven percent of the selected signs on I-285 are found to be good using the proposed method. So, the GDOT inspectors may only focus on the remaining 33% that are in the poor or the uncertain category to visually assess and determine if they require replacement or other corrective actions (such as cleaning). Overall, the proposed method can potentially reduce the GDOT engineers' inspection efforts by approximately 60% and reduce their exposure to unsafe assessment conditions on the road.

SIGN RETO-INTENSITY CHANGE ANALYSIS (2015 – 2018)

LIDAR technology not only helps in assessing the sign retroreflectivity condition, but also in analyzing the retroreflectivity change (deterioration) behavior. Multi-year LIDAR cloud data can be used to establish and analyze the change in sign reflectivity conditions over time and, thus, give insights to the overall deterioration behavior. This section presents a few examples of sign retroreflectivity deterioration behavior from 2015-2018 by analyzing the signs' retro-intensity data. The key statistics of the signs' retro-intensity (median, 25th percentile, and 75th percentile) are captured once every year, and they are plotted to see how these statistics change over the years. For this study, I-285 is selected as the test corridor and signs of different types and colors are studied. **Figure 4-13** shows the different signs and their retro-intensity behavior. From **Figure 4-13** , it is seen that the retro-intensity increases suddenly for all signs in one of the years except for **Figure 4-13** (d). It can be presumed that this sudden rise in retro-intensity is due to the signs' being cleaned intentionally by maintenance teams or by rainfall. It is important to note that dirt on a sign can reduce the retro-reflectivity by more than 20 percent; cleaning a sign can raise the retro-reflectivity by 20 percent.

The Georgia Tech research team conducted an analysis by conditioning a prismatic sign sheet with dirt. Water mixed with dirt in the ratio of 10:1 was applied on the sheet and allowed to dry for 5 hours. This was to simulate the dirt that accumulates on a sign. The average 4-point sign retro-reflectivity measured was 158 cd/lx/m^2 at the beginning of the experiment, and after the conditioning, the average 4-point sign retro-reflectivity dropped to 119 cd/lx/m^2, a drop of 24%.
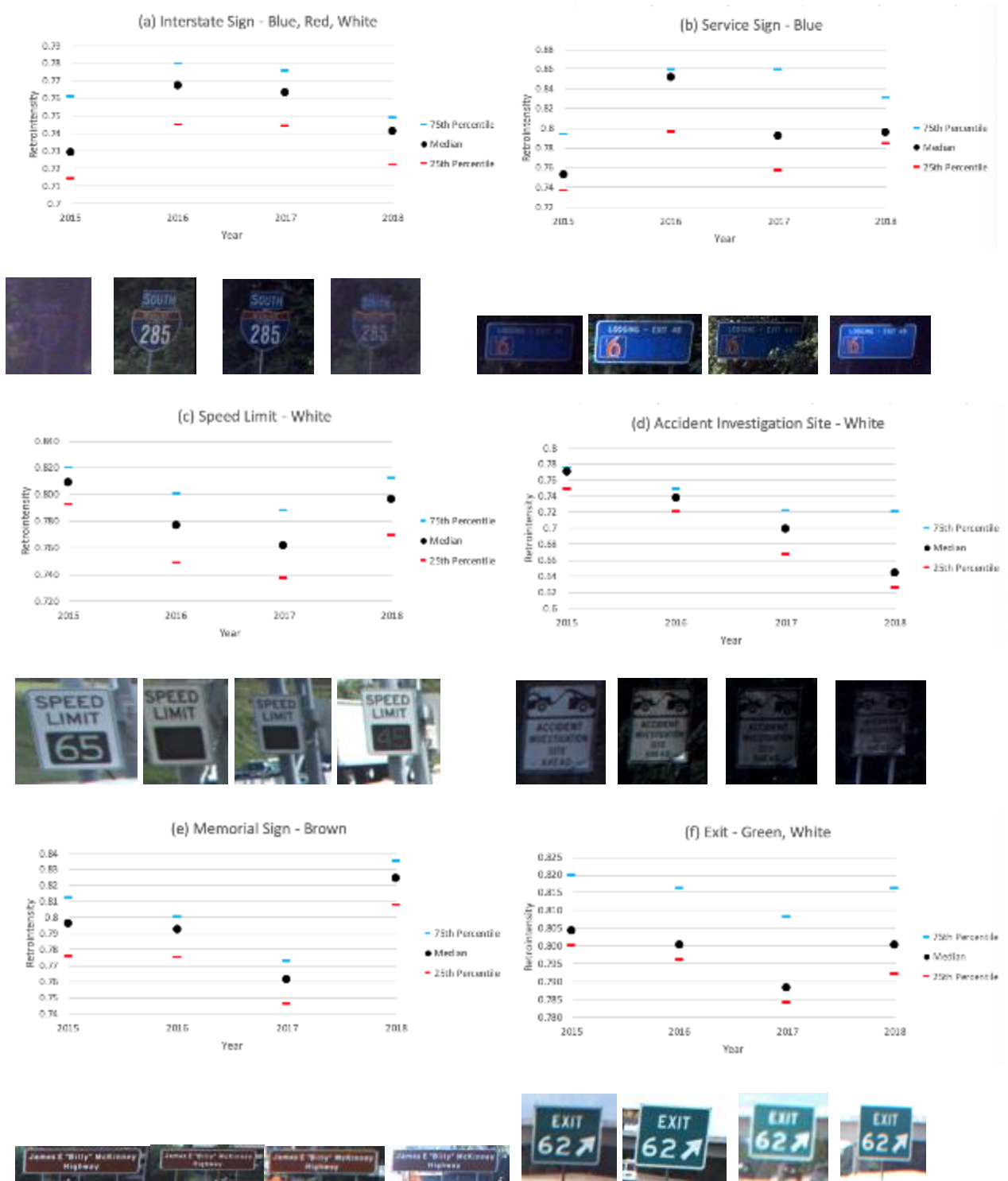
Figure 4-13. Multiple Elements. Retro-intensity deterioration trends from 2015 to 2018 for six selected signs on I-285.

This experiment shows that dirt can significantly reduce the retro-reflectivity. By analyzing the signs in **Figure 4-13** that have a retro-intensity rise in one of the years, it is seen that the retro-intensity rise is less than 20 percent of its previous value, confirming some form of sign cleaning has caused the retro-intensity to go up. Alternatively, the "accident investigation" sign that shows continuous deterioration in **Figure 4-13** (d) is reproduced in **Figure 4-14**.

Figure 4-14. Multiple Elements. Retro-intensity over four years for white sign.

The photos obtained for this sign shows four consecutive years of deterioration without interruption by the cleaning operation. Based on this data, the predicted rate of retro-intensity deterioration is -0.066 per year. However, as evidenced in the photos from 2017 and 2018, the surface of the sign seems to be obscured by dirt. Because of this, it is not

clear how much of the decrease in retro-intensity can be attributed to natural deterioration of the sheeting and how much is solely due to the sheeting being blocked by mud.

Overall, it is promising to observe the signs' retro-intensity deterioration behavior for more years beside the one year of cleaning, especially where retro-intensity increases suddenly. Due to the unpredictable factors of dirt accumulation and sign cleaning, deterioration behavior may not be conclusive for the field sign deterioration analysis without consistent measurement (such as cleaning before each retro-intensity measurement). To determine the deterioration behavior of sign sheeting outside of the influence of dirt, an analysis must be done under controlled and consistent conditions to yield more consistent results.

SUMMARY

The following is a summary of sign retro-reflectivity study using mobile LiDAR:

o   Traffic sign retro-reflectivity is important because it conveys crucial navigation information of the roadway to drivers at night; this information enables drivers to drive safely.

o   There are many challenges with current sign retro-reflectivity condition assessment methods (the nighttime visual inspection method and the retroreflectometer measurement method). They are labor-intensive, time-consuming, dangerous to the workers, involve subjective human assessment, and are constrained by available assessment time (only at night) for visual inspection, or constrained by limited sampling points for the retroreflectometer method. Because of the time-consuming nature of these assessment methods, sign retro-reflectivity condition assessments are

typically only done once per year, so low retroreflectivity signs may stay up for quite

a long time without being replaced. An alternative to individual sign assessments, the

blanket replacement method is simple because it replaces all signs and ensures their

retro-reflectivity values are above the required levels; however, this method is not

economical because some signs may not need replacing.

o Sign retroreflectivity condition data collection using mobile LIDAR is quicker (data

collected at 100 km/h), safer (no need to stop for each sign at the side of the road),

more efficient (data can be collected any time of the day), objective (does not require

a human's subjective assessment, such as nighttime visual inspection), captures more

points (typically greater than 100) than the 4-points sign retro reflectivity

measurements, and is cost-effective. A new method is developed to assess the sign

retroreflectivity condition category (good, poor, uncertain) using the sign's point

cloud data collected by the LIDAR technology. The two main steps involved in this

method include 1) computing the retro intensity statistics (such as median and 25th

percentile) for the sign point cloud data, and 2) classifying the sign retro-reflectivity

condition category (good, poor, uncertain) based on the proposed minimum retro-

intensity (MR) criteria. MR is defined as the retro-intensity value at which the

retroreflectivity meets the minimum MUTCD requirement and is obtained by

correlating the retro-intensity with retro-reflectivity measurements.

o The proposed method was validated using the nighttime visual inspection using signs

collected from GDOT. The assessment was performed by a GDOT inspector who

classified the signs as "acceptable" or "unacceptable" based on the retroreflectivity.

All the signs that failed the nighttime visual assessment method were correctly

classified as "poor" by the proposed method; among the signs that passed, three signs were categorized as "uncertain" due to localized defects on the sign, such as dirt, cracking, and graffiti.

o A case study was performed on I-285 to assess the feasibility of the proposed method by collecting LIDAR data on selected interstate traffic signs. Among 338 selected signs, 67% of the signs were classified as "good", and 33% of the signs were classified as "poor" or "uncertain". From this case study's results, we can clearly see that GDOT can potentially reduce sign retroreflectivity condition assessment effort by approximately 60% on I-285 by screening out the "good" retro-reflectivity signs. GDOT inspectors may only need to assess the remaining 40% of signs in the "poor" and "uncertain" category to determine if they require replacement or cleaning.

o Finally, a study was conducted to assess the retroreflectivity deterioration behavior of selected signs using the retro-intensity data collected on them over the past 4 years. Promising trends for retro-intensity behavior change can be observed on few signs. However, due to the unpredictable factors of dirt accumulation and sign cleaning, the deterioration trends may not be consistent when analyzed for all the signs in the field. Dirt reduces the retro-intensity statistics, and cleaning increases the retro-intensity statistics. Therefore, it is recommended that the retro-intensity deterioration analysis be performed under controlled conditions (clean the signs before retro-intensity measurement) to yield more consistent results.

o Autonomous vehicles constantly collect LIDAR data for their navigation. In the future, it will be possible to assess the sign retro-reflectivity condition dynamically by using the proposed method to collect LIDAR data gathered by autonomous vehicles.

Moreover, using crowd- sourced dynamic sign retroreflectivity condition assessment data from multiple autonomous vehicles making multiple runs along a route, a traffic sign's retro-reflectivity condition for that route can be frequently monitored and replaced proactively when the retroreflectivity drops below required levels.

CHAPTER 5.   ASPHALT PAVEMENT CONDITION EVALUATION

DISTRESSES DEFINED IN PACES

GDOT's statewide pavement maintenance budgeting and programming are based on its pavement condition evaluation system, which provides essential data for determining treatment methods, estimating costs, and selecting projects. Since 1986, GDOT has conducted annual pavement condition evaluations on its entire 18,000-centerline-miles of state routes based on the PACES survey (GDOT, 2007), which was developed by GDOT. PACES was enhanced and upgraded to the COPACES in 1998 (Tsai & Lai, 2002), a paperless system that enhanced data quality and improved the efficiency of the field data collection system. COPACES surveys were performed by GDOT's engineers during the winter (September to February) without having to employ additional resources. The past manual surveys conducted using COPACES involved recording the severity and extent of various types of pavement surface distresses, including cracking, rutting, raveling, potholes, etc. For cracking, a 100-foot representative section was selected for a detailed walking survey to determine the severity and extent of distresses; the section would represent the 1-mile segment (GDOT, 2007). For other distresses, a windshield survey was carried out over a continuous 1-mile segment. The distresses recorded for all the segments (which are typically one-mile long, except for the first and last segment) are aggregated/averaged to obtain the representative pavement condition for a project (typically several miles long). A COPACES rating (on a scale of 0 to 100 with 100

representing a pavement in excellent condition) is then computed based on the extent and the severity level of each distress for each segment and project. To enable uniform, impartial data collection and reporting across Georgia, COPACES establishes standardized nomenclature for distresses and defines their respective severity levels and measurement method. There are ten distresses surveyed in COPACES. They are rutting, load cracking, block cracking, reflective cracking, raveling, edge distress, bleeding/flushing, corrugation/pushing, loss of section, and patches/ potholes, as listed in **Table 5-1Error! Reference source not found.**. The distress types are categorized and associated with potential causes of the pavement defects, so the data can be used for determining the treatment method. For example, longitudinal cracking and fatigue cracking occurring within the wheel path are considered as load-related cracking (i.e., load cracking), and block cracking is considered as non-load-related cracking due to aging and weathering.

Table 5-1. Asphalt pavement distresses defined in COPACES.

Distress	Unit	Severity	Survey Length
Load Cracking	%	1, 2, 3, 4	100-foot
Block Cracking	%	1, 2, 3	100-foot
Reflection Cracking	Number, Foot	1, 2, 3	100-foot
Edge Distress	%	1, 2, 3	1-mile
Rutting	1/8 inch	-	100-foot
Patches/Potholes	Number	-	1-mile
Bleeding	%	1, 2, 3	1-mile
Raveling	%	1, 2, 3	1-mile
Corrugation	%	1, 2, 3	1-mile
Loss of Section	%	1, 2, 3	1-mile

Due to the advancement of sensing technology and the shortage of internal manpower, GDOT has started to outsource its statewide pavement condition survey. However, the distress protocol defined in PACES needs to be preserved in order to make sure the new data consistent with the historical data. In this project, the extracted pavement condition data is fully compatible with PACES. Thus, the results can also be used by GDOT to compare with the data acquired from an outsourced contractor.

STREAMLINED PROCEDURE

The streamlined procedure for asphalt pavement condition evaluation has been applied in previous project (RP 15-11), which was continuously used in this project. To improve the accuracy of raveling detection and classification, an enhanced QA/QC procedure was adopted. The following introduction in this subsection is included in the final report of RP 15-11. However, to make this report a self-contained one, the introduction is still kept in this final report.

The streamlined procedure for pavement condition evaluation follows GDOT's COPACES survey method. The procedure utilizes both the automated methods for pavement distress extraction (including cracking, rutting, and raveling) and several customized interactive tools for the extraction of other characteristics. **Figure 5-1Error! Reference source not found.** shows the flowchart of the proposed procedure, which consists of five primary steps. The QA/QC steps are used to guarantee the quality of the extraction results. Since the automatic results are generated covering all the interstate highways using the interval of a frame in the sensing data collection (i.e., 5 m), the steps of the COPACES boundary identification and COPACES rating generation steps were

proposed to summarize the automatic results into a COPACES reporting unit, i.e.,

segments and projects. New reporting segments and projects are generated for the

locations without any previous COPACES reporting.
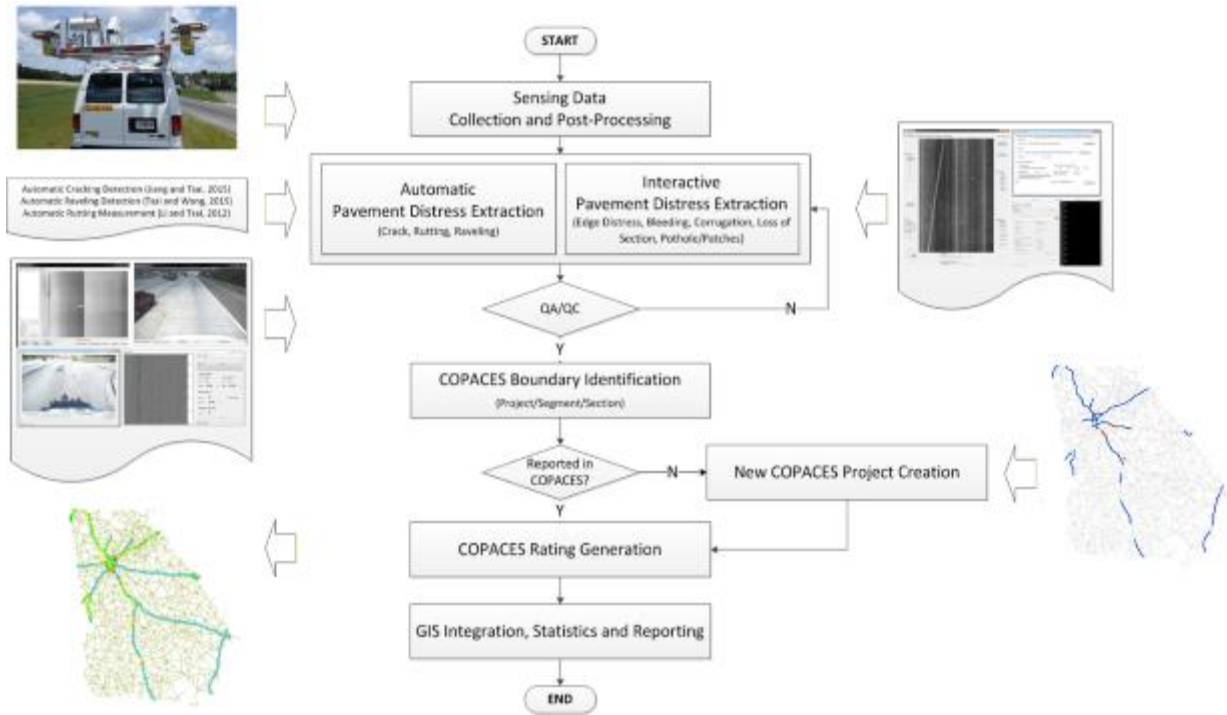
Figure 5-1. Flowchart. Streamlined procedure for asphalt pavement data collection

and processing. (Jiang & Tsai, 2016; Tsai, 2015; Tsai & Wang, 2014; Tsai & Li,

2012).

COPACES Reporting using Automatic Results

Because the automatic results are reported based on the interval of data frame acquisition,

i.e., a 5-m interval, the COPACES reporting from the automatic results requires spatial

correlation and aggregation. Especially for cracking (including load crack, block crack

and reflective crack), the COPACES reporting is generated based on a 100-foot

representative section within the survey segment. Therefore, two procedures were proposed for spatially correlating the COPACES survey segments and for aggregation and selection of the representative 100-foot section.

Spatial correlation for COPACES survey segments

The collected sensing data are geo-referenced using accurate GPS coordinates so that the results of automatic pavement distress extraction are also geo-referenced with the same GPS coordinates. First, the pavement surface type is identified for all the interstate routes using the geo-referenced image frames. After spatially joining each data frame to GDOT's linear referencing system, comprised of RCLINK and mile point, a map is created as shown in **Figure 5-2Error! Reference source not found.** to define the pavement type of interstate routes as either asphalt concrete, JPCP, or CRCP. In summary, the data collected cover a total of 1,250 centerline miles out of which 54.8% are asphalt concrete, 38.0% are JPCP, and 7.2% are CRCP. In this chapter, asphalt concrete pavements are selected for further analysis. Next, the selected data frames are matched to their corresponding COPACES segments identified in the project RP 15-11. The segments are then aggregated according to the projects defined by the COPACES dataset. All the projects that are greater than 10 miles are double-checked to ensure the pavement conditions and characteristics are homogeneous within the limit. Therefore, after filtering out corrupted and missing data, more than 400,000 frames were used to compute the COPACES rating of the interstate asphalt pavement segments and projects.
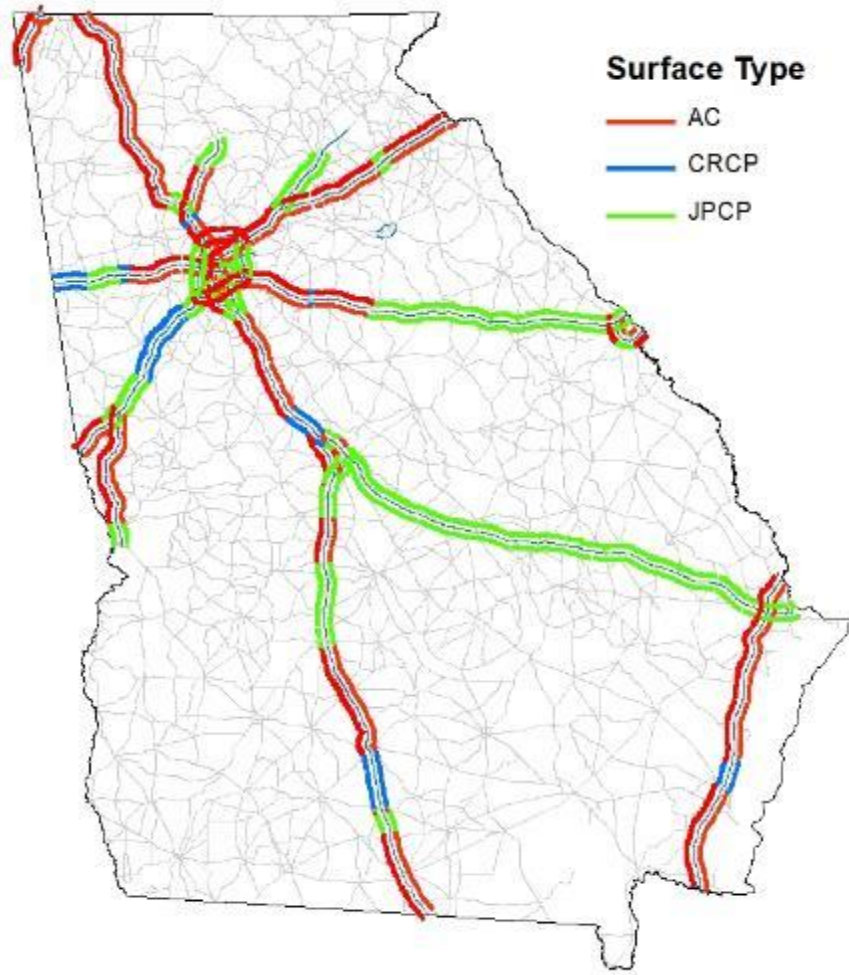
Figure 5-2. Map. Georgia's interstate pavement surface type.

100-foot representative section aggregation and selection for crack survey

 In COPACES, a walking survey is conducted for cracking in a 100-foot representative
sample section in each 1-mile segment. Using the automatic pavement distress extraction
results, the research team reports the detailed difference for each data frame (i.e., 5 m
interval). Therefore, for each 1-mile segment, the automatic results can generate fifty-two
100-foot sections, whereas results from six data frames are aggregated for the
corresponding 100-foot section. **Figure 5-3Error! Reference source not found.**

illustrates the fifty-two 100-foot sections reported within a 1-mile segment. In order to mimic the selection criteria performed by GDOT for a representative section, the deduct value for each individual section is computed, whereas a 60th percentile of the deduct distribution is used for selecting the "representative" section to represent the 1-mile segment. Therefore, the severity level and extent values for the selected "representative" section are used to represent the entire 1-mile segment. The percentile is calibrated by comparing the results from the automatic crack extraction, and the results are manually reviewed by field engineers from GDOT. It is observed that the 60th percentile can best capture the field engineers' judgment in selecting the "representative" section. It should be noted that although a 60th percentile is used to generate the COPACES ratings in this study, the derived results using the automatic distress extraction have the capability to generate a full-coverage, continuous crack severity level and extent values without the need to aggregate them into a "representative" 100-foot section artificially.
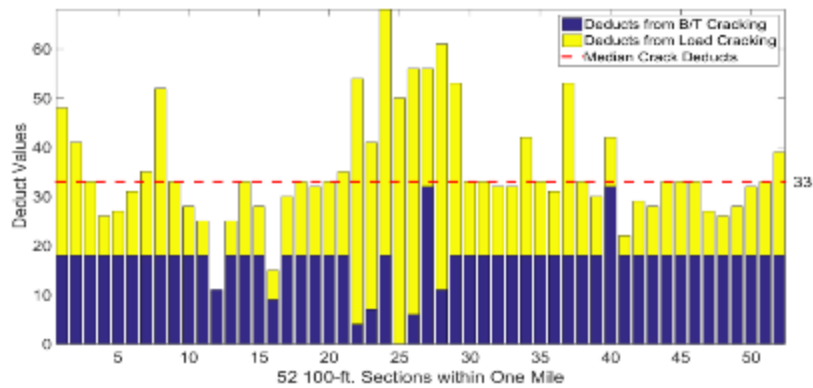
Figure 5-3. Chart. Fifty-two 100-foot sections reported within a 1-mile segment.

71

RESULTS

The COPACES ratings were computed for a total of 1,289 surveyed miles of asphalt pavement data that were collected using the GTSV. **Figure 5-5** shows the mapped results of the derived COPACES ratings. Overall, the pavement condition on interstate highways in Georgia is acceptable, except for a few sections on I-75, I-85, etc. As seen in **Figure 5-5Error! Reference source not found.**, the project ratings range from 60 to 99, with an average rating of 82 for all projects. There are 16 projects with a rating of 70 or below, thus requiring some maintenance action, such as resurfacing.
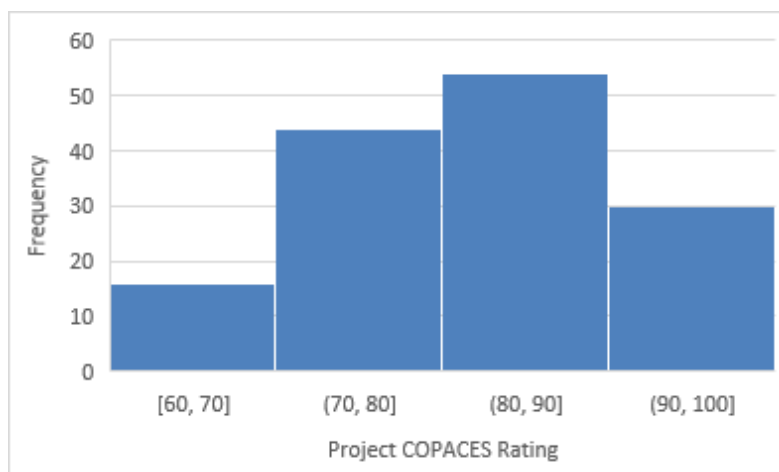
Figure 5-4. Chart. Project COPACES rating histogram.

Detailed COPACES deducts in the major distresses, such as load cracking, block cracking, raveling, and rutting, were further studied. As shown in **Figure 5-6** , it can be observed that the overall deduct values related to load cracking and block cracking are relatively low, most of them being below 6 points; this indicates that a low extent and low severity level are mostly identified along the surveyed pavements. Similarly, rutting

deduct values were mostly below 5 points (i.e. less than ¼ inch). On the other hand, raveling is the major contributor to the project rating reduction with around 75% of the projects having a raveling deduct value of 10 or above, which indicates more than 36% extent are Severity Level 1 or more than 15% are Severity Level 2.
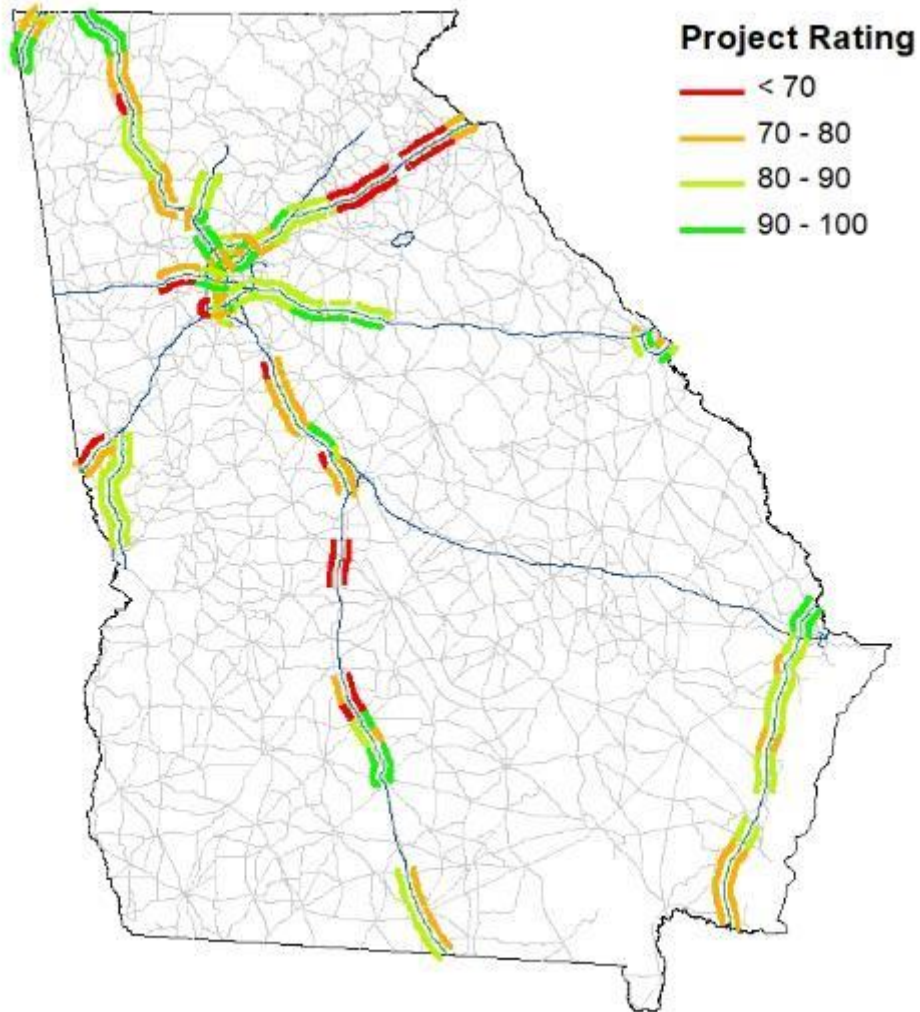
Figure 5-5. Map. Derived COPACES ratings using the proposed method.
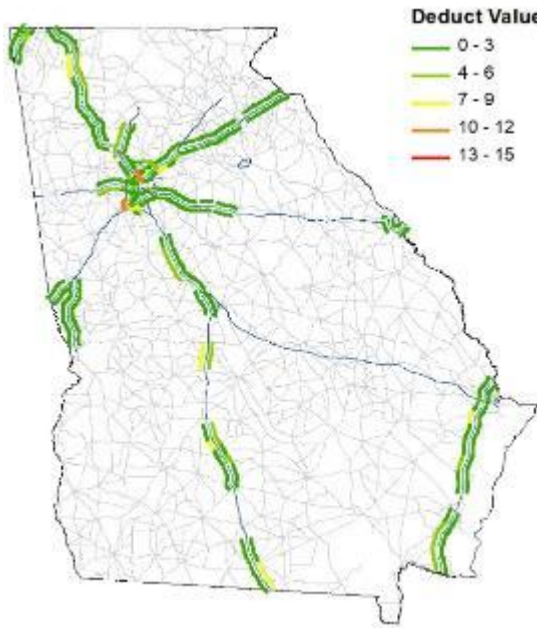
A. Subfigure of load cracking deduct values map
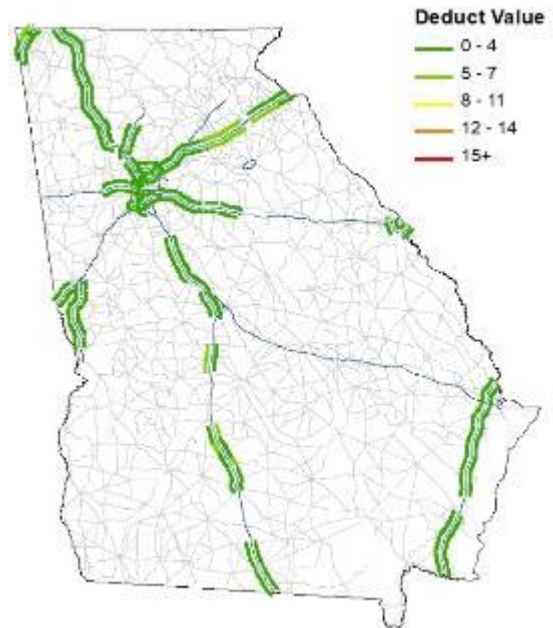
B. Subfigure of load cracking deduct values map
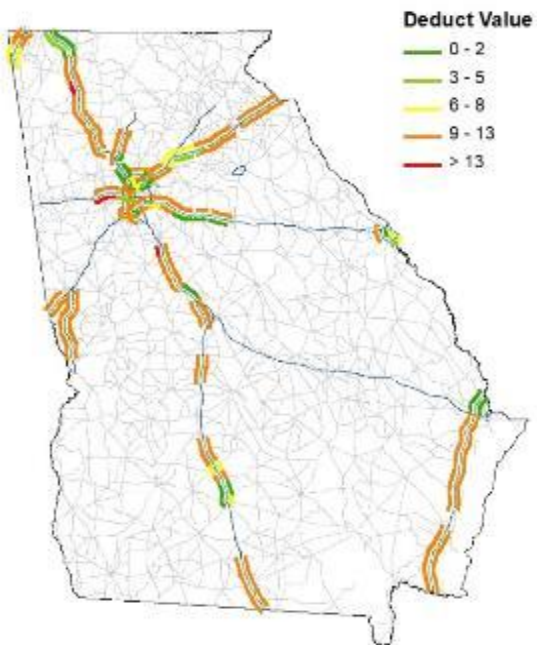
C. Subfigure of raveling deduct values map
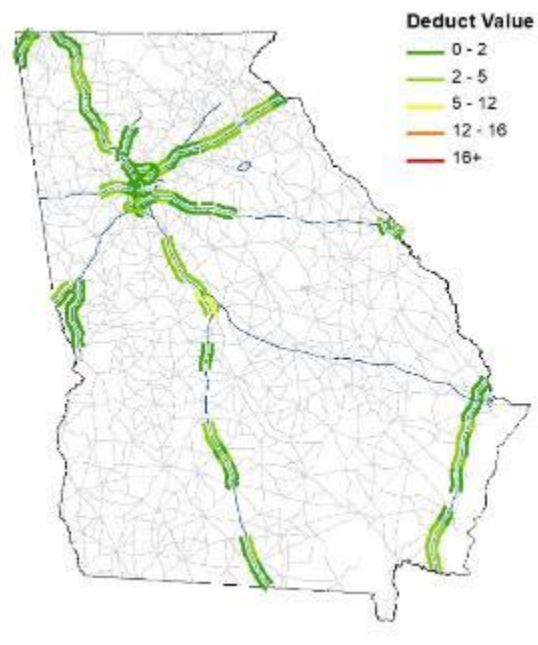
D. Subfigure of rutting deduct values map

Figure 5-6. Maps. Major pavement distresses' deduct values.

COMPARISON WITH 2015 PAVEMENT CONDITION DATA

By comparing the results obtained in a previous GDOT research project, RP 15-11, we notice that the average rating has dropped from 85.6 to 82. This shows that the network level condition is dropping and more funding may be required. Raveling continues to be the major contributor to the reduction in project ratings. **Figure 5-7** shows the comparison of COPACES project ratings derived using the same method for 2015 and 2018.
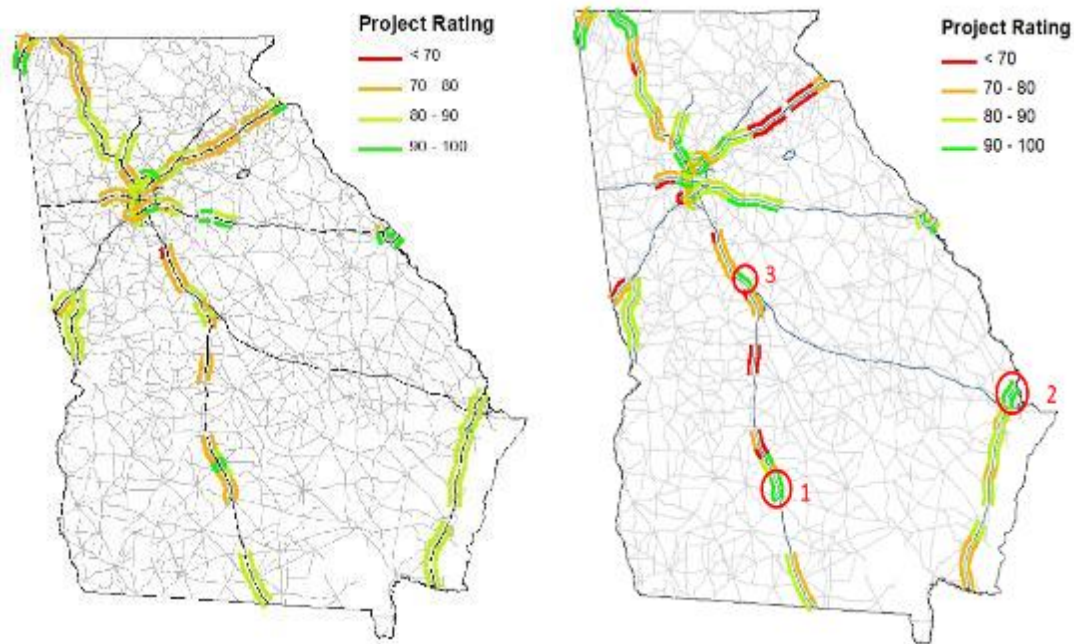
A. Subfigure of 2015 Map   B. Subfigure of 2018 Map

Figure 5-7. Maps. Comparison between 2015 and 2018 Project Ratings.

As shown in the above maps, the project ratings have dropped as expected at different rates depending on several factors affecting pavement deterioration behavior such as design, traffic, climate, etc. On the other hand, an increase in project rating was also noticed for projects where resurfacing or some form of maintenance has been performed.

Three spots where a noted increase of rating between 2015 and 2018 were highlighted in **Figure 5-7** (B) for further analysis. **Figure 5-8** shows the comparison of images collected using GTSV for 'Spot 1' located on I-75 south-bound where complete resurfacing has been performed over the project length and road width. **Figure 5-9** shows the 2018 images of 'Spot 2' located on I-95 NB and SB where partial resurfacing has been performed for selected segments. **Figure 5-10** shows an image comparison of 'Spot 3' located on I-75 NB near Macon where partial resurfacing has been conducted on the truck lane only.

A. Subfigure of 2015   B. Subfigure of 2018

Figure 5-8. Photos. Comparison of spot 1 northbound resurfacing between 2015 and 2018.

A. Subfigure of 2018 NB   B. Subfigure of 2018 SB

Figure 5-9. Photos. Spot 2 northbound and southbound partial resurfacing.

A. Subfigure of 2015   B. Subfigure of 2018

Figure 5-10. Photos. Comparison of spot 3 northbound truck lane resurfacing

between 2015 and 2018.

SUMMARY

By using the streamlined method for pavement condition evaluation, a comprehensive rating was performed for all asphalt pavement projects on interstate routes. As a result, the network condition was shown to be acceptable with an average rating of 82 for all projects; however, this is a drop from 85.6 in 2015. Thus, more funding and maintenance optimization is required to improve the network-level project rating.

CHAPTER 6.   PCC PAVEMENT (JPCP) CONDITION EVALUATION

OVERVIEW OF JPCP AND RATING SYSTEM

GDOT currently maintains 783 centerline miles of rigid pavements on Georgia's states routes, mainly on the interstate highways (GDOT, 2017). The rigid pavements account for merely 4.36% of the entire state route network of 17,959 miles. However, they play a critical role in freight transportation, as they carry more than 20% of Georgia's truck traffic (Tsai, 2016). Rigid pavements include continuously reinforced concrete pavement (CRCP) and jointed plain concrete pavement (JPCP). Eighty-nine centerline miles of CRCP and 475 centerline miles of JPCP total 564 centerline miles of rigid pavements on Georgia's interstate highways. Around 84% of rigid pavements are JPCP, and most of these JPCP were built between 1958 and 1986. Since many of them are reaching the end of their service lives, JPCP condition assessment survey is critical for their maintenance, rehabilitation, and reconstruction (MR&R); it is also important for identifying budget needs. GDOT has conducted JPCP condition evaluations since the 1970s based on its concrete pavement condition evaluation system (CPACES), which was revised in the 1990s to standardize the JPCP survey in terms of distress types and severity levels. In 2016, an enhanced JPCP Condition Evaluation System (JPCPACES) was developed by the Georgia Tech research team to better monitor the severe distresses of aged JPCP (Tsai & Wu, 2019). Surveys conducted using JPCPACES involve recording 11 categories of JPCP distresses and pavement roughness (IRI) in the outside lane at 1-mile intervals. A JPCPACES rating scale of 0 to 100 (with 100 representing excellent condition) is

computed based on 8 out of 11 categories of distresses and IRI, shown with bolded words in **Table 6-1**. The purposes of recording 3 categories of distresses in JPCPACES is to predict how many slabs will be replaced and to evaluate the performance of replacement materials, though these 3 distresses didn't directly contribute to deduction points. To be noted is that when counting broken slabs, JPCPACES didn't differentiate original or replaced slabs. So, all the failed slabs actually impact the rating.

Table 6-1. JPCPACES Survey Distresses.

Distress Type	Sample Location	Severity	Unit
Faulting	Every 8th joint	-	Faulting Reading (1/32")
Slabs with transverse crack	1 mile	Level 1	# of slabs
		Level 2	
Slabs with longitudinal crack	1 mile	Level 1	# of slabs
		Level 2	
Corner break	1 mile	-	# of slabs
Shattered slab	1 mile	-	# of slabs
Replaced slab	1 mile	-	# of slabs
Failed replaced slab	1 mile	-	# of slabs
Joint with spalls	1 mile	-	# of joints
Joint with patched spalls	1 mile	-	# of joints
Joint with failed spalls patches	1 mile	-	# of joints
Shoulder joint distress	1 mile	-	% of mile
Roughness (IRI)[1]	1 mile	-	mm/km

Note: (1) Faulting is collected using a Georgia Faultmeter (GFM).

(2) Roughness is collected by the Laser Profiler.

JPCPACES ratings are calculated using a maximum score of 100 and minus 6 deduct values. These 6 deduct values are combined from 8 categories of distresses and IRI. The combination and calculation can be found in the following function and annotations:

$$Rating = 100 - D_{FI} - D_{SM} - D_{CS} - D_{LC} - D_{SD} - D_{SP}$$

Where:

- D_{FI}: Deduct value for Faulting Index

- D_{SM}: Deduct value for Smoothness

- D_{CS}: Deduct value for Cracked Slabs (consist of slabs with transverse cracks, corner break slab and shattered slab)

- D_{LC}: Deduct value for Longitudinal Cracks

- D_{SD}: Deduct value for Shoulder Distress

- D_{SP}: Deduct value for Spalls (consist of joint with spalls and Joint with failed spall patches)

STREAMLINED PROCEDURE USING 3D PAVEMENT DATA

In this study, JPCP condition assessment was conducted by using full-coverage, high-accuracy 3D pavement data. The pavement distresses were detected, classified, and measured using a semi-automatic method. The condition rating system follows the current JPCPACES. However, in comparison with the traditional windshield-based or walk-through methods, the new method is much faster, more objective, and accurate. Meanwhile, to leverage the advantages of the full-coverage and high-accuracy 3D pavement data, some of the previous limitations will be enhanced. In the traditional walk-through method, faulting is only measured at every eighth transverse joint using a GFM in order to reduce the labor effort. By using the full-coverage, high-accuracy 3D pavement data, we can now measure faulting at each single joint, which should be more accurate than the previous walk-through method.

Nevertheless, the processing of 3D pavement data is complicated. By employing both automatic and manual processes, we have developed a streamlined procedure for data processing. The streamlined procedure, as shown in **Figure 6-1**, aims to improve the productivity and reliability of data processing. The procedure consists of five primary steps, including 1) sensing data collection and post-processing, 2) JPCP identification, 3) Joint detection, 4) JPCP distress extraction and 5) JPCPACES rating computation. In the procedure, several automatic tools are used to conduct data post-processing, joint detection, IRI calculation, and joint faulting calculation. QA/QC steps are used to guarantee the quality of the automatically extracted results.
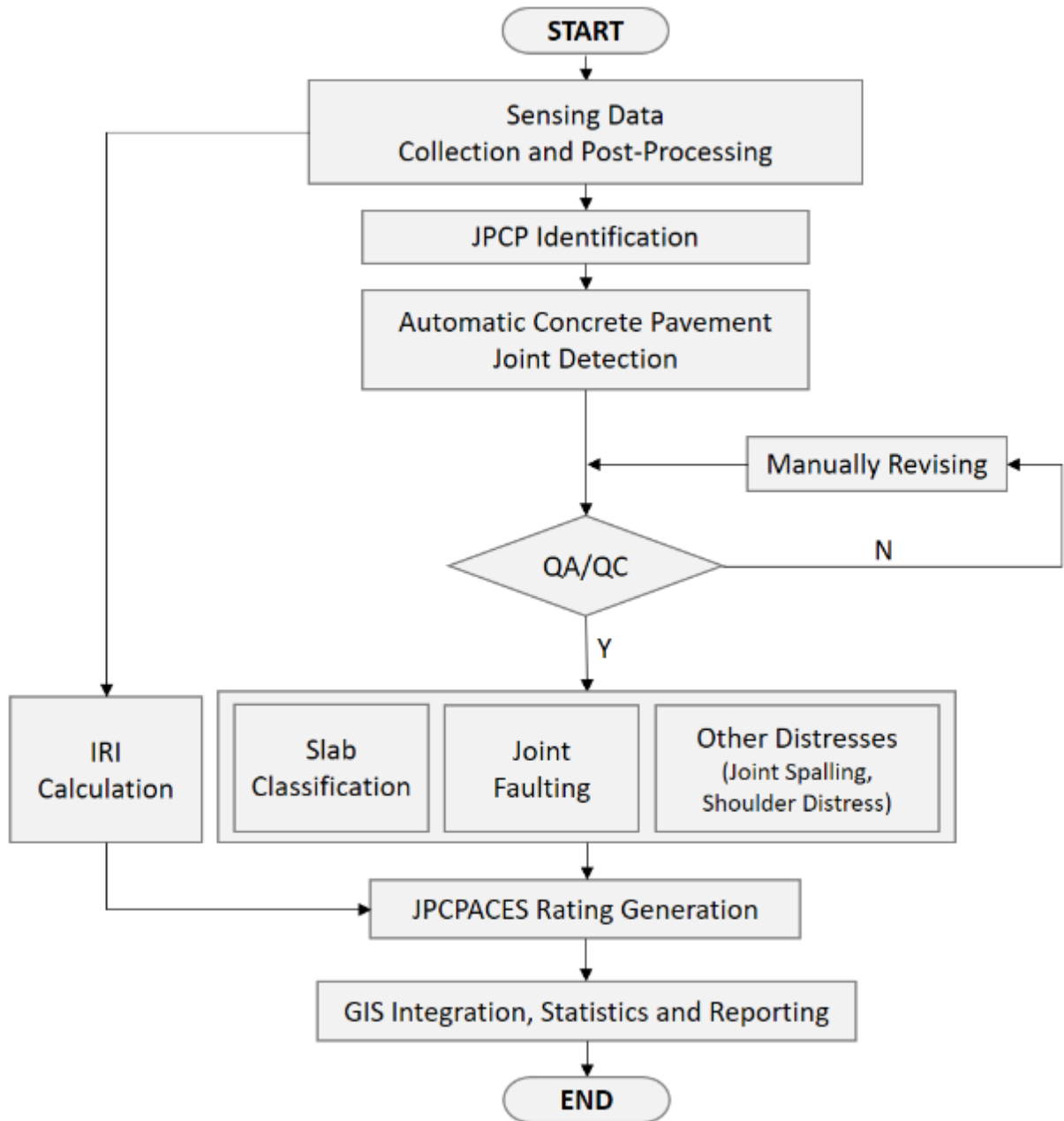
Figure 6-1. Flowchart. Streamlined procedure for JPCP 3D pavement data processing.

3D JPCP Data Collection

As previously mentioned, the GTSV is used for collecting 3D pavement data. Although 3D pavement data processing and analysis progress were divided into two parts (one for asphalt pavement and another for JPCP), data collection tasks were not separated for different types of pavement. For example, I-75 south of Atlanta has combined asphalt data, JPCP and CRCP, which were continuously collected in one day. However, additional efforts were needed to separate the collected data in terms of different types of pavement. The results showed there are 564 centerline miles of PCC pavement on Georgia's interstate highways, which consist of 475 centerline miles of JPCP and 89 miles of CRCP. After JPCP data are separated, more than 300,000 frames of 3D JPCP pavement images need to be processed for joint identification, distresses extraction, and IRI measurement.

Joint Identification for JPCP Data

Since JPCP is designed with contraction joints to control the location of expected cracks, JPCPACES is a slab-based rating system. The joints between two adjacent slabs need to be accurately identified. Thus, the total number of slabs in each mile can be accurately determined and the deductions of broken slabs can be computed. In addition, the accuracy of a joint location is also very critical for area-based faulting calculation using 3D pavement data. For this reason, both an automatic joint-detection tool and a manual QA/QC tool were developed to ensure the efficiency and accuracy of joint detection.

JPCP Distress Extraction Method

Though the JPCP distress extraction method has been changed from a windshield survey to automated 3D-pavement-data-based method, the distress extraction is still consistent with GDOT's JPCPACES. However, enhancement has been made to facilitate the use of full-coverage, highly accurate 3D pavement data. For example, the exact crack length had been defined to differentiate Level 1 and Level 2 longitudinally- and transversely-cracked slabs. In addition, some limitations of windshield and walkthrough surveys were overcome by leverage the full-coverage, highly accurate 3D pavement data. For example, a faulting index traditionally measured by a Georgia Faultmeter (GFM) required traffic control, which results in only one-eighth of the joints being collected to represent the average faulting index. With the full-coverage 3D pavement data, the faulting at each joint can be conveniently measured. The following briefly introduces the extraction/measurement of different JPCP distresses using 3D pavement data.

Faulting Index

 Full-coverage, continuous 3D JPCP data is used to calculate the faulting value. Unlike the field measurement using a GFM, which only measures one point in the right wheel path at every eighth joint for a 1-mile segment, the automated method measures 24 faulting values at each joint for each 1 mile. Each faulting value is calculated by the difference of average height in two 50 mm $\times$ 100mm square area with 60 mm from each side of the joint. These 24 areas are evenly distributed between two-lane markings. The calculated result is the actual height difference in millimeters, which is different from the existing unit of the faulting index for calculating deduct values. For this reason, a new table for transferring the actual faulting height to the faulting index was developed. As

mentioned in the JPCPACES manual, the faulting index 20 is equivalent to 3.2 mm of average faulting value, which has a 19 deduct value. The detailed measurement procedures are introduced in Geary's paper (Geary, Tsai & Wu, 2018).

Slab Classification

To improve the efficiency and consistency of slab classification, the definitions of different categories of broken slabs have been enhanced. The enhanced definitions are more objective than the previous ones due to the use of quantitative crack lengths for each category of cracked slabs. For example, at Severity Level 1, the longitudinally cracked slab is defined as the one with longitudinal crack longer than 1 ft that starts at a transverse joint; and the Severity Level 2 is defined as the one with longitudinal crack longer than 75% of the slab length. Meanwhile, a decision flowchart has been developed for slab classification. For example, if a longitudinal Severity Level 2 longitudinal crack and a Severity Level 1 transverse crack occurred simultaneously, this flowchart will check whether it is a shattered slab or not, and then check if it is a Severity Level 2 longitudinally cracked slab; it will finally check if it is a Severity Level 1 transversely cracked slab. This flowchart is more logically intact and could avoid some of the ambiguity in previous definitions.

Joint Defects

There are three types of joint defects visually inspected in a JPCPACES survey. They are joints with spall, joints with patched spalls, and joints with failed spall patches. However, only joints with spall and joints with failed spall patches were counted for calculating the deduct value of joint defects according to JPCPACES. In this study, joint defects are manually identified during the slab classification and QA/QC processing

using 3D pavement data. The criteria for identifying joint defect are consistent with JPCPACES.

Shoulder Distress

Previously, shoulder distresses were visually inspected based on their severity, and there are two severity levels defined in JPCPACES. The "pumping" of the base material is a key criterion for visual inspection to identify the severity level. However, pumping material is difficult to discern in 3D pavement data. Therefore, in this research, only joint depth and joint width are considered as rules to identify shoulder distresses and classify the severity levels.

RESULTS

In this study, the JPCPACES ratings were computed for 988 survey segments, and each segment represented 1 mile. The overall JPCP condition of Georgia's interstate highways is relatively acceptable with an average rating of 83.7 for all segments. There are 178 segments with a rating below 70 and which potentially need maintenance or replacement. The poor performing JPCP are located at I-85 north of Atlanta, I-20 west of Atlanta, I-20 east of Atlanta from MP 130-MP 150, I-16 near Macon and I-16 from MP 80-MP 90.

JPCPACES ratings were plotted for each 1-mile segment in **Figure 6-2**. The detailed six categories of deducts, such as the deduct value for the faulting index, smoothness, cracked slabs, longitudinal cracks, shoulder distress, and joint spalls were further plotted separately in **Figure 6-3** and **Figure 6-4**. From the plotting results, the deduct value for the faulting index is highly correlated to the deduct value for IRI, which indicates the

faulting index greatly impacts a vehicle's ride quality, and it is necessary to apply

diamond grinding in those certain segments. Moreover, it is found that the high deduct

value for longitudinal cracks was mostly concentrated on I-20 west of Atlanta.   The high

deduct value for shattered slabs was evenly distributed in all the segments with low
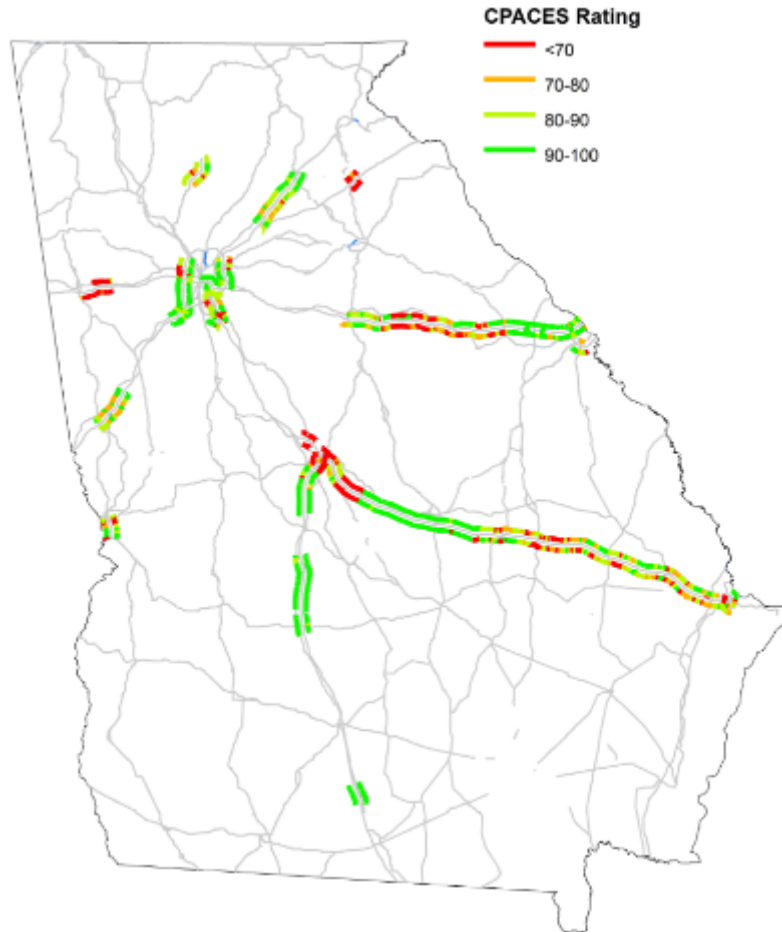
JPCPACES ratings.

Figure 6-2. Map. Derived JPCPACES rating using 3D pavement data.
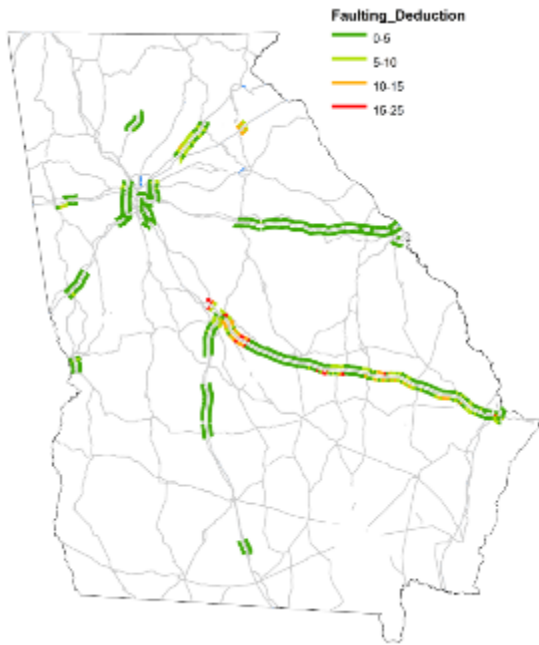
A. Faulting deduct values map
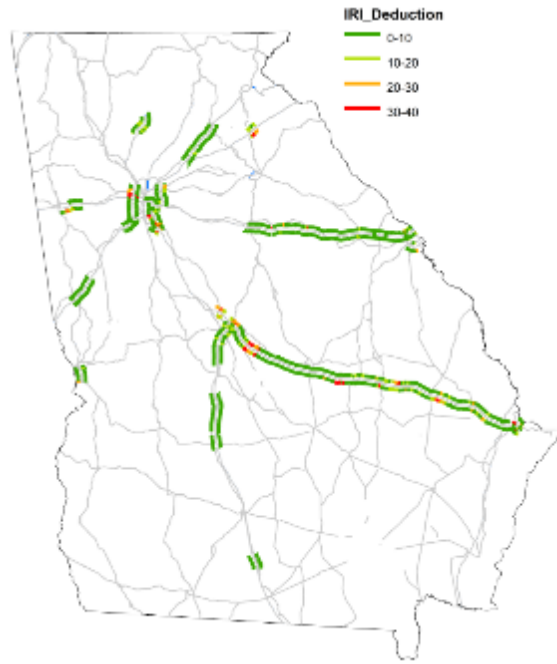
B. IRI deduct values map
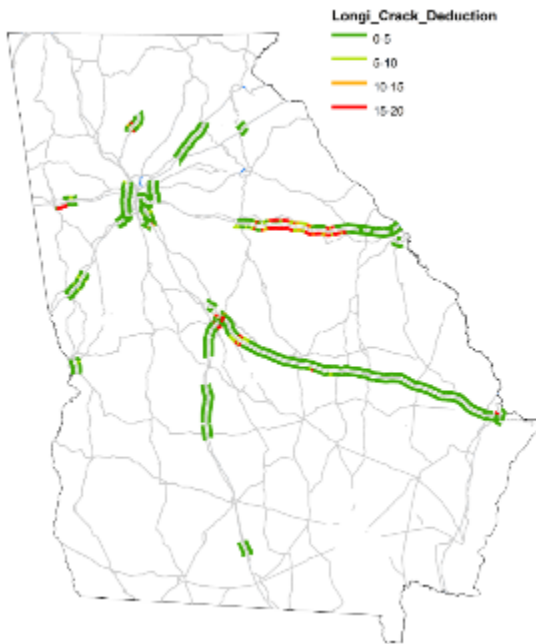
C. Long. cracking deduct values map
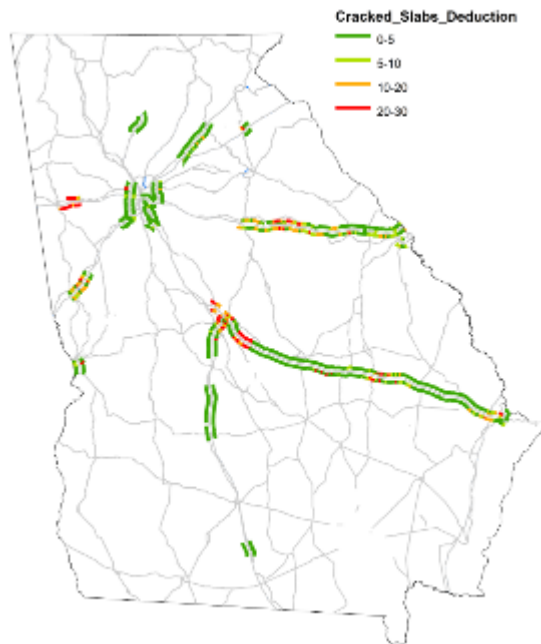
D. Cracked slabs deduct values map

Figure 6-3. Maps. Major JPCP distresses' deduct values.
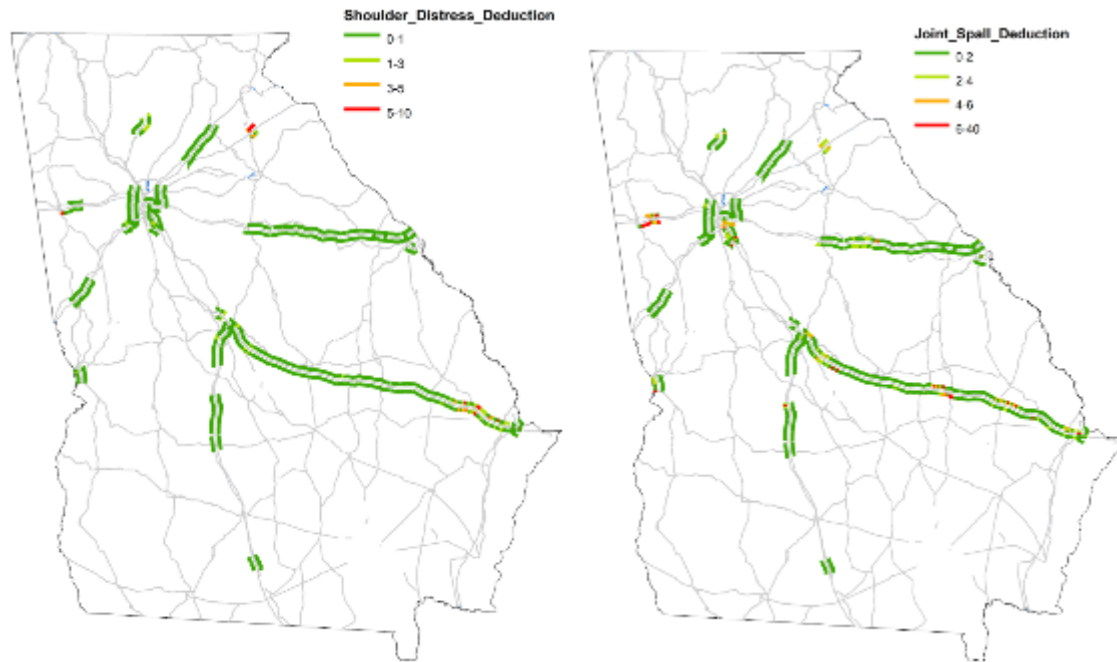
A. Shoulder distress deduct values map   B. Joint Spalling deduct values map

Figure 6-4. Maps. Major JPCP distresses' deduct values (continued).

COMPARISON WITH HISTORICAL CPACES RATING

The subsection compares the current JPCPACES rating (GT-2018-JPCPACES) with the historical CPACES rating (GDOT-Historical-CPACES).

To compare the overall pavement condition on each interstate highway containing JPCP, the average overall rating, faulting, IRI, the percentage of shoulder distress and the number of T1, T2, L1, L2, SS, CC, and joint spall are summarized in the following **Table 6-2** for both GT-2018-JPCPACES and GDOT-Historical-CPACES, respectively. The following summarize observations.

Table 6-2. Comparison between GT-2018 JPCPACES rating and GDOT historical rating.

Type	Route	Start - End	Rating	Avgs. Fault (mm)	Avgs. IRI (m/km)	Avgs. T1 BS L1 (#)	Avgs. T2	Avgs. SS	Avgs. CC	Avgs. L1 (#)	Avgs. L2 (#)	Joint Spall (#)	Shoulder (%)
							Broken Slabs Level 2 (#)						
GT_2018	I20	MP113 - MP201	73.2	0.76	1.14	2.0	6.6	5.3	0.6	9.6	17.4	6.8	0.2
CPACES_2016			84.4	0.71	1.03	6.1	0.6			21.3	0.7	1.8	0.0
GT_2018	I985	MP0 - MP24	87.3	1.67	1.21	1.0	1.4	0.2	0.2	0.9	0.3	0.4	0.1
CPACES_2017			89.3	1.48	0.90	10.8	0.9			10.3	1.0	0.3	0.0
GT_2018	I16	MP0 - MP166	80.3	1.35	1.36	0.7	3.3	2.2	0.5	0.7	1.4	6.4	1.5
CPACES_2016			93.8	1.46	1.24	1.8	0.5			0.8	0.4	0.8	0.9
GT_2018	I675	MP0 - MP9	81.4	0.88	1.53	0.6	1.3	0.5	0.8	1.5	0.6	13.8	3.5
CPACES_2015			90.0	1.11	1.48	0.0	0.0			0.0	0.0	3.0	0.0
GT_2018	I520	MP5 - MP9	80.5	0.89	1.48	0.3	5.4	0.8	0.5	0.4	0.1	7.8	1.9
CPACES_2016			90.1	0.54	1.26	3.7	0.1			0.4	0.0	0.0	0.0
GT_2018	I185	MP0 - MP9	83.1	1.04	1.45	0.6	1.1	1.4	0.4	1.6	1.9	8.6	2.1
CPACES_2016			94.1	0	1.24	1.2	0.2			1.3	0.0	1.6	0.0
GT_2018	I85	MP150 - MP155	53.7	2.28	1.79	0.7	3.3	1.3	1.1	0.7	1.1	20.4	3.8
CPACES_2017			66.4	2.28	1.76	7.7	3.3			3.0	0.8	15.6	0.0
GT_2018	I75	MP31 - MP40 &	89.3	0.65	1.20	0.3	1.7	0.6	0.1	1.0	0.3	3.9	0.2
CPACES_2017		MP98 - MP164	93.0	0	1.12	2.5	0.7			0.2	0.0	0.0	0.0

The GT-2018-JPCPACES rating is usually lower than GDOT-Historical-CPACES rating for each route. For example, I-16 and I-20 of GT-2018-JPCPACES rating are 73.15 and 80.33, which are lower than 84.4 and 93.8 of GDOT-2016-CPACES rating, respectively.

The average faulting and IRI are usually similar between GT-2018-JPCPACES rating and GDOT-Historical-CPACES rating, though the data collection methods are not the same. For example, I-20 has a relatively low value of average faulting and IRI compared to I-16, so both GT-2018-JPCPACES rating and GDOT-2016-CPACES rating gave a low value of average faulting and IRI for I-20 but gave a high value of average faulting and IRI for I-16.

The average number of total cracked slabs (including T1, T2, L1, L2, SS, CC), joint of spall and the average percentage of shoulder distress from GT-2018-JPCPACES results usually greater than GDOT-Historical-CPACES results, except the locations where

pavement maintenance was conducted (e.g. I-985 had slab replacement before Dec. 2018).

The GDOT-Historical-CPACES is more likely to count L2 as L1 and broken slabs level 2 as broken slabs level 1. For example, GT-2018-JPCPACES results indicated an average of 9.55 L1/mile and 17.37 L2/mile but GDOT-2016-CPACES revealed an average of 21.3 L1/mile and 0.73 L2/mile on I-20. The same situation also happened for broken slabs. GT-2018-JPCPACES results shown average 1.97 broken slabs level 1 (T1)/mile and average 12.56 broken slabs level 2 (T2 + SS + CC)/mile, but GDOT-2016-CPACES shown average 6.11 broken slabs level 1/mile and 0.57 broken slabs level2. This is probably due to the difference in survey procedure between GT-JPCPACES and CPACES. As slab classification method mentioned above in JPCPACES distress extraction paragraph, the enhanced slab classification method is more objective compared to the traditional subjective CPACES.

CHAPTER 7.   SMOOTHNESS EVALUATION USING 3D PAVEMENT DATA

METHOD FOR IRI MEASUREMENT USING 3D LASER DATA

Chapter 2 described the procedure for 3D pavement data collection, which was used to estimate the pavement's international roughness index (IRI). The IRI for the left and right wheelpaths using the quarter-car model, as well as the half-car roughness index (HRI) was calculated (Sayers, 1989) for each 1-mile segment by the following steps:

1) The longitudinal pavement profile was extracted from the 3D pavement data.

2) A low-pass filter of 30Hz was applied to mitigate high-frequency noise from the obtained profile.

3) The filtered longitudinal profile was saved in a .ppf format. This is a commonly used format used for pavement profile information and is compatible with ProVal.

4) The IRI for the left and right wheelpaths and HRI was calculated from the filtered longitudinal profile data for each 5-meter interval.

5) The IRI value estimates for each 1-mile segment were aggregated to provide the IRI value for that segment.

The following sections present the IRI validation procedure to ensure that the values of IRI obtained from the GTSV are reasonable. The first assessment is the major one through which a rigorous and quantitative field validation was performed by comparing GTSV to GDOT laser profilers in GDOT's asphalt and concrete IRI calibration and validations sites. The second assessment was a qualitative validation by comparing

GTSV with Pathway's IRI data to make sure the trend is reasonable. However, note that the purpose of the latter section is not to evaluate the quality of Pathway's IRI data.

FIELD VALIDATION WITH GDOT'S PROFILER

Validation of the method for IRI measurement was completed by comparison with IRI values obtained using AASHTO R56 (AASHTO, 2014) and certified GDOT Profilers (**Figure 7-1**) on the GDOT test sections. The GDOT Profilers comprised a system of 7 laser scanners affixed to the front bumper of a vehicle, which captured a thin longitudinal profile of the pavement surface used to estimate the IRI.

Figure 7-1. Photo. GDOT Profiler.

On February 14, 2019, pavement condition data was collected using both the GDOT profiler and the GTSV on two test sections (one asphalt and one concrete). The asphalt test section was located inside Middle Georgia Regional Airport near Macon, Georgia, (**Figure 7-2** (b)) and the concrete test section was located on U.S. Route 41 near Barnesville, Georgia (**Figure 7-2**(a)). The test sections were 0.1 mile (528 feet) long, with 500-foot buffers on each side. The test sections were marked with reflective tape, as

shown in figure **Figure 7-2** (b), which would be easily visible in both the GDOT

profiler's longitudinal profiles as well as the range images from the GTSV's laser scanner.

The end points of the buffers were marked with traffic cones (**Figure 7-2** (a)). Each test

section was covered in multiple runs by both the GDOT Profiler and the GTSV.

A. Subfigure of concrete test section   B. Subfigure of asphalt test section

Figure 7-2. Photos.Test sections for IRI validation.

First, the repeatability of the IRI estimates from data collected using the GTSV was

evaluated. Each test section was collected in 10 runs using the GTSV. The runs were

manually registered to align them by locating the reflective strip at the start of the test

section in the intensity images for each run. The IRI was then estimated. The IRI

estimated from each run for the left and right wheelpaths from the asphalt test section is

given in **Figure 7-3**. Run 7 was omitted as the vehicle path was askew during that run.

Qualitatively, the repeatability of the estimated IRI can be observed especially in the

features at Segments 13-23 in the left wheel path and Segments 13-22 in the right wheel

path. Quantitatively, the Pearson correlation between each series of IRI values derived

from each run was calculated. As shown in **Figure 7-4**, there is generally a high

correlation between any two runs, with an average correlation of 0.7912 for the left wheel

path and 0.7876 for the right wheel path.
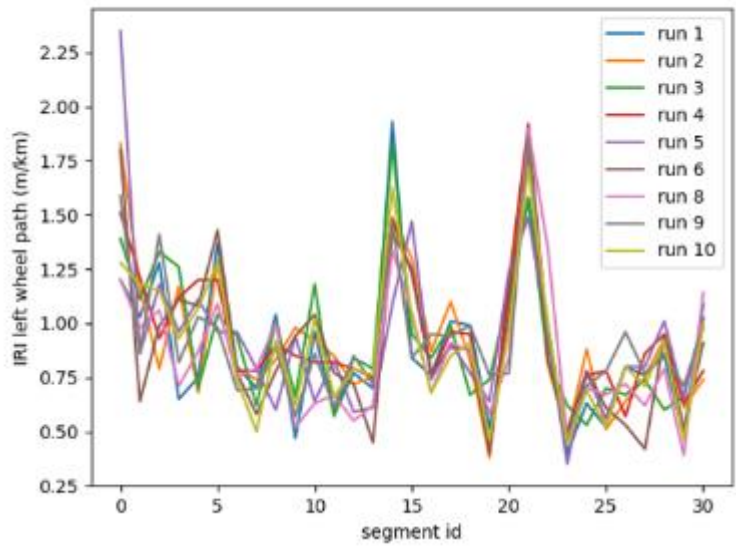
A. Subfigure of left wheel path
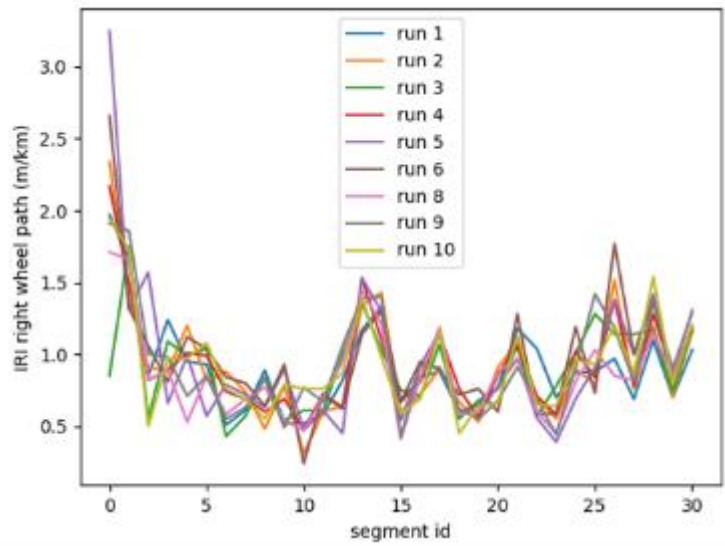
B. Subfigure of right wheel path

Figure 7-3. Graphs. IRI estimated using GTSV data.

A. Subfigure of left wheel path

B. Subfigure of right wheel path

Figure 7-4. Graphs. Correlation between IRI estimated from different GTSV runs.

Second, the accuracy of IRI estimation using the GTSV was evaluated. GDOT provided

the longitudinal profiles collected using the GDOT Profilers, which were used to

determine the IRI for each wheelpath individually using ProVal. As the GDOT Profilers

were certified, this can be considered as the ground truth IRI values. Similarly, the IRI

was estimated using runs of data collected using the GTSV. The calculated IRI from each

device is given in **Table 7-1**. The difference between the average IRI estimates is -0.58

in/mi for the left wheel path and 2.57 in/mi for the right wheel path. These are generally

very low error values. To put these values in context, the ride quality classifications for

different IRI values as defined by the Federal Highway Administration (FHWA) and the

New York State Department of Transportation (NYSDOT) are given in **Figure 7-5**. It can

be observed that the slab size for the classification levels is much larger than the

differences in IRI values estimated by the profiler and the GTSV. Thus, it can be

concluded that the GTSV provides an accurate estimate of the pavement IRI for the

purposes of pavement condition assessment and maintenance.

Table 7-1. IRI from GDOT profiler and GTSV.

Run	GDOT IRI left (in/mi)	GTSV IRI left (in/mi)	GDOT IRI right (in/mi)	GTSV IRI right (in/mi)
1	62.16	62.07	61.13	62.57
2	63.06	61.38	62.01	61.60
3	63.13	63.63	60.86	64.17
4	63.26	64.42	60.63	65.72
5	62.87	61.91	61.37	64.83
6	63.35	60.92	61.86	64.38
Average	**62.97**	**62.39**	**61.31**	**63.88**

IRI (in/mi)	<60	60-94	95-119	120-144	145-170	171-194	196-220	>220
FHWA Interstates	V.Good	Good	Fair	Mediocre		Poor		
FHWA Other	V.Good	Good	Fair			Mediocre		Poor
NYSDOT	V.Smooth	Smooth		Fair		Rough		V.Rough

Figure 7-5. Matrix. Rid quality classification by FHWA and NYSDOT.

COMPARISON WITH PATHWAY DATA

Pathway data was used to estimate the IRI for a test section on I-85 northbound (MP34-57) from 2013-2015. This section compares the IRI estimated using this data with IRI estimates using the GTSV in 2017-2018. Although the years do not have any overlap, the IRI does not change drastically over this time duration, as shown in **Figure 7-6**.
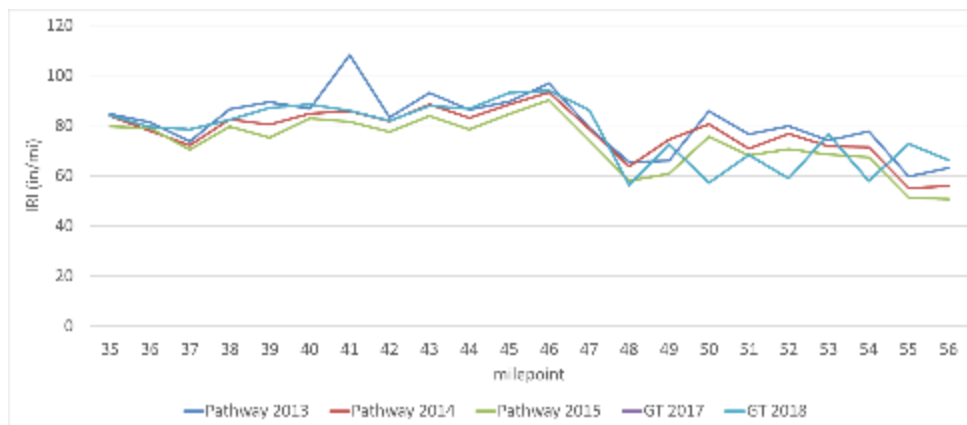

Figure 7-6. Graph. IRI obtained from Pathway and GTSV.

GTSV data from 2017 and 2018 were compared. The average standard deviation between the IRI values estimated for each mile was 4.65 in/mi, with the highest standard deviation occurring at MP 41-42 of 9.51 in/mi.

PROCESSED RESULTS FOR INTERSTATE HIGHWAY

The HRI was processed for all the interstate routes collected by the GTSV, including both asphalt and concrete pavements, and the results were mapped as shown in **Figure 7-8**. HRI values were computed for each 1-mile segment along the route and displayed according to the categories defined by FHWA IRI requirements shown in **Figure 7-5**, which were multiplied by 0.8 to obtain the corresponding HRI categories (Sayers, 1989). As shown in **Figure 7-7**, 78% of the interstate fell into the "Very Good" and "Good" categories defined by FHWA with an HRI value of less than 76 in/mile, with few exceptions of higher HRI on I-16.
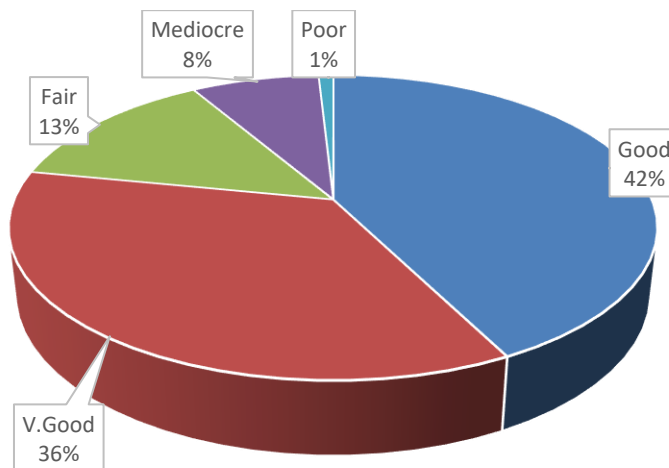
Figure 7-7. Chart. Georgia Interstates HRI distribution according to categories defined by FHWA.
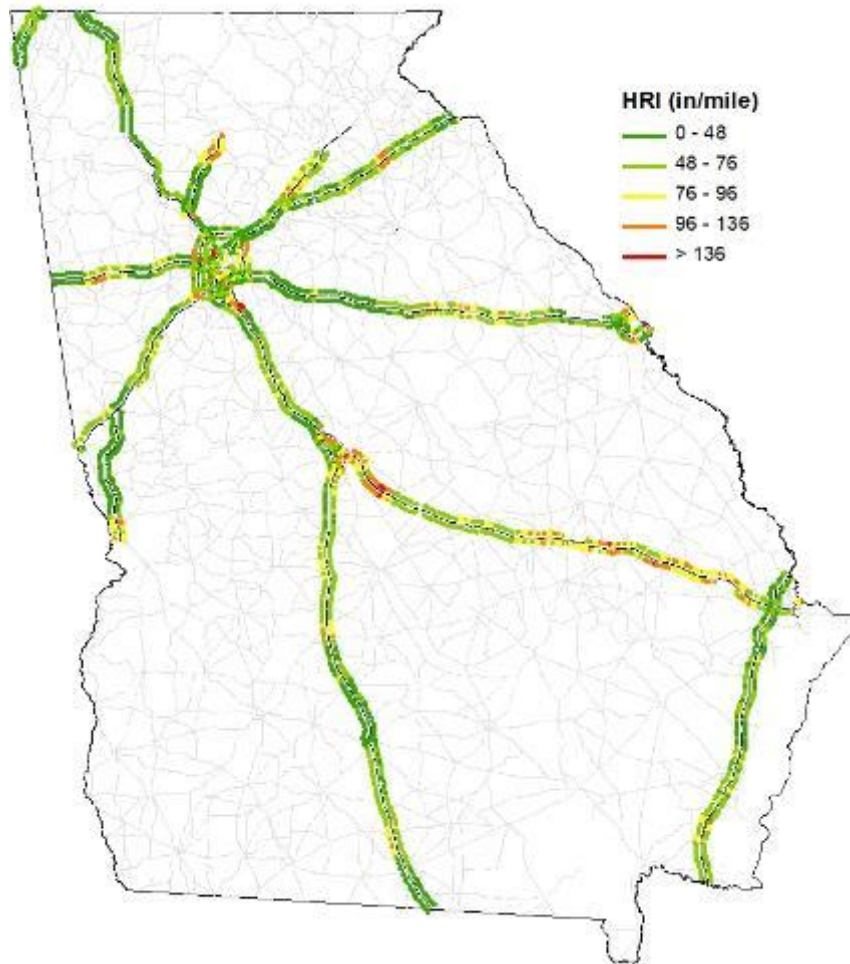
Figure 7-8. Map. HRI measurements of Georgia's interstate routes.

SUMMARY

In this chapter, the method for processing IRI was described. Validation tests for
processing IRI were conducted in February 2019 with Qutais Hannah, Jimmy Norwood,
and Nathan Johnson of the Office of Materials and Testing. A comparison with historical
IRI data from Pathway was also conducted. After processing the HRI values for all
interstate routes, most of them were categorized as either "Very Good" or "Good"
according the criteria defined by FHWA.

CHAPTER 8. CONCLUSIONS AND RECOMMENDATIONS

CONCLUSIONS

As a continuous effort of the previous research project (RP 15-11), this research project conducted sign inventory and condition assessment on Georgia's interstate highways using 2D imaging and 3D LiDAR. A novel mobile-LiDAR-based sign retro-reflectivity condition assessment method was also validated, and a case study using selected signs on I-285 was conducted to demonstrate the feasibility of the proposed method. Through this research project, it is further confirmed that the proposed method is very promising and can provide a cost-effective means for sign inventory and retro-reflectivity condition assessment using 2D imaging and 3D LiDAR. After the completion of the first GDOT-sponsored research project (RP 15-11), which showcased the successful implementation of 3D technology to evaluate the pavement condition of Georgia's interstate highways, it has helped promote the adoption of this technology nation-wide. Thus, a survey reported in 2017 shows that eighteen states have already adopted the 3D automated data collection system, and seventeen states have indicated that they plan to use it within the next two years (NCHRP 501, 2017). This project further proves the abilities of this technology and justifies the need to proceed with its implementation as a cost-effective method for pavement condition survey. As a result, in this research project, asphalt pavement condition evaluation, PCC (JPCP) pavement condition evaluation, and IRI measurement was conducted on the entire Georgia's interstate highways using 3D sensing technology. Overall, it helps advance GDOT's pavement management system by enhancing the

accuracy of Georgia's interstate long-term maintenance and rehabilitation planning and programming. The following summarize the major findings from this research project.

Sign inventory and condition assessment

- There were 21,427 traffic signs inventoried in 2018 along all the interstate highways using a procedure that makes use of previously collected data (2015 Sign Inventory). The guide signs make up 65% (13,969 signs) of the total sign population on the interstate. The rest of the population consists of 4,465 regulatory signs, 2,717 warning signs, and 276 other signs (temporary signs and signs with no identifiable MUTCD codes).

- There are 1,256 signs (6% of the overall traffic sign population) in poor conditions (such as surface failure, post failure, obstructed by vegetation, and dirty) that require maintenance . Surface failure of the signs make up the largest number of signs in poor condition in 2018; this is followed by signs that are dirty. The next two cases are signs that are obstructed, and signs whose posts failed. Further studies are needed to determine the number of signs in poor condition in 2015 that were not repaired until 2018 and to determine the number of additional signs that dropped into poor condition

- There are 4,135 overhead signs (19% of the overall traffic sign population). They have a high potential risk of failure and require frequent monitoring and condition assessment.

- There is an increase of 1.87% in the number of signs in the 2018 Sign Inventory compared to the 2015 Sign Inventory. The largest increase in a number of signs is

attributable to regulatory signs (4%, 188 signs). One of the noted reasons for change in this category comes from the "Prohibited Holding Mobile Devices While Driving" signs. These signs were installed after 2015 when the state of Georgia passed the Hands-Free Georgia Law (HB673). The increase in the number of signs in 2018 is also due to 102 signs on I-516 in Savannah, Gorgia that were not counted in the 2015 Sign Inventory.

Sign retro-reflectivity condition assessment

- A new method was developed to assess the sign retro-reflectivity condition category (good, poor, and uncertain) using a sign's point cloud data collected by mobile LIDAR technology. The two main steps involved in this method include 1) computing the retro intensity statistics (such as median and 25th percentile) for the sign point cloud data, and 2) classifying the sign retro-reflectivity condition category (good, poor, uncertain) based on the proposed minimum retro-intensity (MR) criteria.

- The proposed method was validated using the nighttime visual inspection method and by using sign data collected by GDOT. The assessment was performed by a GDOT inspector who classified the signs as "acceptable" or "unacceptable" based on the retro-reflectivity. All the signs that failed the nighttime visual assessment method were correctly classified as "poor" by the proposed method; among the signs that passed, three signs were categorized as "uncertain" due to localized defects on the sign, such as dirt, cracking, or graffiti.

- A case study was performed on I-285 to assess the feasibility of the proposed method by collecting LIDAR data of selected interstate traffic signs. Among 338 selected

signs, 67% of the signs were classified as having good retro-reflectivity, and 33% of the signs were classified as "poor" or "uncertain" retro-reflectivity. Using this result, the GDOT inspectors only had to focus on the remaining 33% that were in the poor or the uncertain category to visually assess and determine if they require replacement or other corrective actions (such as cleaning). Overall, the proposed method can potentially reduce the GDOT engineers' inspection efforts by approximately 60% and reduce their exposure to unsafe assessment conditions on the road.

- A study was conducted to assess the retro-reflectivity deterioration behavior of selected signs using the retro-intensity data collected on them in the past 4 years. Promising trends for retro-intensity behavior change can be observed on few signs. However, due to the unpredictable factors of dirt accumulation, rains, and cleaning of signs by the maintenance crews, the deterioration trends may not be consistent for all the signs in the field. Therefore, it is recommended that the retro-intensity deterioration analysis be performed under controlled conditions (cleaning the signs before retro-intensity measurement) to yield more consistent results.

Asphalt Pavement Condition Assessment

- The COPACES ratings were computed for 1,289 miles of asphalt pavement by using the streamlined method for asphalt pavement condition evaluation.

- Overall, the pavement condition on interstate highways in Georgia is acceptable, except for a few sections. The project ratings range from a low of 60 to a high of 99, with an average rating of 82 for all projects. There are 16 projects with a rating of 70 or below that require maintenance.

- The overall deduct value related to load cracking and block cracking are relatively low, most of them being below 6 points, indicating that a low-extent and low-severity level is mostly identified along the surveyed pavements. Similarly, the rutting deduct values were mostly below 5 points, indicating an average rutting of below ¼ inches. However, raveling is the major contributor to the project rating reduction with around 75% of the projects having a raveling deduct value of 10% or above, which indicates more than 36% extent of Severity Level 1, or more than 15% at Severity Level 2.

PCC (JPCP) Pavement Condition Assessment

- The JPCP ratings (JPCPACES) were computed for a total of 988 survey segments, and each segment represented 1 mile. The overall JPCP condition on Georgia's interstate highway is relatively acceptable with an average rating of 83.7 for all segments. There are 178 segments with a rating below 70, which potentially indicates a need for maintenance or replacement. The poor performance JPCP segments are located at I-75 north of Atlanta, I-20 west of Atlanta, I-20 east of Atlanta from MP 130-MP 150, I-16 near Macon and I-16 from MP 80 to MP 90.
- The deduct value for the faulting index is highly correlated to the deduct value for IRI, which indicates the faulting index greatly impacts the ride quality. Moreover, it is found that the high deduct value for longitudinal cracks was mostly concentrated on I-20 west of Atlanta. The high deduct value for shattered slabs was evenly distributed in all the segments with low JPCPACES ratings.

Smoothness Evaluation

- The validation of the method for IRI measurement was conducted by comparing the IRI values obtained by using the GTSV and by using a GDOT Profiler on two GDOT test sections. First, the repeatability test of the GTSV resulted in a high correlation between any two runs with an average correlation of 0.7912 for the left wheel path and 0.7876 for the right wheel path. Second, the difference of the average IRI collected by the GTSV and a GDOT profiler is -0.58 in/mi for the left wheel path and 2.57 in/mi for the right wheel path, which shows a high accuracy of IRI measurement using the GTSV.

- The GTSV data from 2017 and 2018 were compared with the data collected by Pathway on I-85 northbound (MP 34 – MP 57). The average standard deviation between the IRI values estimated for each mile was 4.65 in/mi, with the highest standard deviation occurring at MP 41-42 of the 9.51 in/mi section.

- The HRI was processed for all the interstate route data collected by the GTSV, including both asphalt and concrete pavements. Seventy-eight percent of the interstate fell into the "Very Good" and "Good" categories according to the FHWA definition with an HRI value of less than 76 in/mile; there were a few exceptions of higher HRI, mainly on I-16.

RECOMMENDATIONS FOR IMPLEMENTATION

Sign Inventory and Condition Assessment

5) GDOT can take proactive action using the research outcomes from this project to locate and perform timely maintenance for the signs in poor condition in each district. Based on the sign inventory outcomes, along with conditions, it is recommended that GDOT districts use the research outcomes (different categories of poor sign conditions and their locations) to actively perform maintenance and replacement to ensure roadway safety. If the districts are limited by resources for maintenance, it is recommended they perform the maintenance and replacement on the regulatory signs first.

6) GDOT can also use the collected interstate highway sign inventory from this research project to assist the GDOT Office of Transportation Data (OTD) in performing QA/QC on the current statewide sign inventory effort.

7) From the results of I-285 case study on selected signs, we can clearly see that GDOT can potentially reduce sign retro-reflectivity condition assessment effort by approximately 60% on I-285 by screening out the "good" retro-reflectivity signs. GDOT inspectors may only need to assess the remaining 40% of signs in the "poor" and "uncertain" categories to determine if they require replacement or cleaning. To validate the accuracy of the results, it is recommended that GDOT verify the research outcomes from the I-285 case study by assessing the selected signs in the field with its inspectors and perform cleaning or replacement actions on the signs that were identified as "poor" or "uncertain."

8) It is further recommended that GDOT implement the sign retro-reflectivity condition assessment as proposed in this research project at the network-level using the safe, cost-effective mobile-LiDAR data collected at highway speed after the field validation.

Pavement Condition Assessment

5) Knowing that GDOT has a new production operation with an outsourced, automated collection method using 3D sensing technology, it is recommended that a quality assurance procedure be developed to ensure the data quality needed to support the MR&R decision-making. Validating the accuracy and reliability of the GTSV in pavement condition evaluation shows a great potential for use by GDOT as a rigorous method to evaluate the data quality provided by the vendors as part of the data quality management plan.

6) It is recommended that the high granularity of 3D pavement surface data be leveraged not only for evaluating the network condition, but also for maintenance and rehabilitation decisions at the project level. For example, 100-ft aggregated pavement distresses can be obtained and used for determining coring locations required by the Office of Materials and Testing for pavement design evaluation. Moreover, this data can also be used to define optimal termini for localized maintenance applications, such as deep patching of asphalt pavements, or be used to estimate the quantity of broken slab replacements for JPCP needed.

7) Because of having accurate pavement condition data, it is recommended this 3D and pavement distress data be used to better study pavement deterioration

behavior and develop a reliable pavement performance forecasting model. For example, a raveling deterioration and forecasting study can be developed to improve GDOT's predictive and preventive maintenance, such as fog seal, micro-milling, and thin overlay optimal timing. Similarly, the slab-level pavement distresses of JPCP can be used to study the change of slab conditions and develop accurate forecasting models to support MR&R decisions, including broken slab replacement.

8) After validating the IRI accuracy collected by the GTSV, it is recommended that GDOT use 3D pavement data, already collected for measurement of cracking, rutting, etc. to compute IRI to reduce the additional effort and cost required to compute IRI data using the laser profilers.

REFERENCES

Ai, C. and Tsai, Y. (2014). "Critical Assessment of an Enhanced Traffic Sign Detection Method Using Mobile LIDAR and INS Technologies*." Journal of Transportation Engineering,* 141(5): 04014096.

Ai, C., Tsai, Y. (2016). "Automated Traffic Sign Retroreflectivity Condition Assessment Using Computer Vision and Mobile LIDAR*.", Transportation Research Part C: Emerging Technologies*, Vol. 63, pp. 96-113.

Ai, C., Tsai, Y., Wang, Z., and Yezzi, A.(2017) "Systems and Methods for Identifying Traffic Control Devices and Testing the Retroreflectivity of the Same." U.S. Patent US9767371 B2 (Granted on Sept. 19th, 2017)

Brody, J. (2007). "Growing Older, and Adjusting to the Dark.", (website) The New York Times. Available online: https://www.nytimes.com/2007/03/13/health/13brody.html, last accessed November 1, 2019.

Carlson, P.J., and Lupes, M. S. (2007). *Methods for maintaining traffic sign retro-reflectivity*, Report No. FHWA-HRT-08-026, Federal Highway Administration, McLean, VA.

Federal Highway Administration. (2012). "Minimum Sign Retroreflectivity Requirements." (website) McLean, VA. Available online: https://safety.fhwa.dot.gov/roadway_dept/night_visib/policy_guide/sign_15mins/, last accessed October 15, 2019.

Georgia Department of Transportation (GDOT) Foreman Academy manual (2012).

GDOT (2017). *County Mileage of Public Roads in Georgia by Surface Type for 2017, Report No. 441,* Georgie Department of Transportation, Atlanta, GA.

Geary, G. M., Tsai, Y., & Wu, Y. (2018). "An Area-Based Faulting Measurement Method Using Three-Dimensional Pavement Data." *Transportation Research Record*, 2672(40), 41-49.

Guan, H., Li, J., Yu, Y., Ji, Z., & Wang, C. (2015). "Using mobile LIDAR data for rapidly updating road markings." *IEEE Transactions on Intelligent Transportation Systems*, 16(5), 2457-2466.

McGee, H. W. (2010*). Maintenance of signs and sign supports: a guide for local highway and street maintenance personnel,* Report No. FHWA-SA-09-025, Federal Highway Administration, Washington, D.C.

MnDOT (2014). *Traffic Sign Maintenance/Management Handbook,* Report No. 2014RIC20, Version 2.0, MnDOT Research Services Section, St. Paul, Minnesota.

Tsai, Y., Ai, C., Wang, Z., Pitts, E. (2013). "A Mobile Cross Slope Measurement Method Using LIDAR Technology.*", Journal of The Transportation Research Record*, 2367 (2), pp. 53-59.

Tsai, Y., Ai, C., Wang, Z., Pitts, E. (2013). "A Mobile Cross Slope Measurement Method Using LIDAR Technology.", *Journal of The Transportation Research Record*, 2367 (2), pp. 53-59.

Tsai, Y. J., Wang, Z., & Ai, C. (2017). *Implementation of automatic sign inventory and pavement condition evaluation on Georgia's interstate highways,* Report No. FHWA-GA-16-15-11, Georgia Department of Transportation, Atlanta, GA.

Tsai, Y. J., & Wu, Y. C. (2019). *Developing a Comprehensive Pavement Condition Evaluation System for Rigid Pavements in Georgia*, Report No. FHWA-GA-19-1502, Georgia Department of Transportation, Atlanta, GA.

Ma, Y., Zheng,Y., Cheng, J., & Easa, S. (2019). "Real-time Visualization Method for Estimating Highway 3D Sight Distance Using LIDAR Data." *Journal of Transportation Engineering, Part A: Systems*, 145(4): 04019006.

Zimmerman, K. (2017). *NCHRP Synthesis 501 Pavement Management Systems: Putting Data to Work*, Transportation Research Board of the National Academies, Washington, D.C.